2-1-2020

Enhancing Produce Safety: State Estimation-based Robust Adaptive Control of a Produce Wash System

Vahid Azimi
Georgia Institute of Technology, vahid.azimi@gatech.edu

Daniel Munther
Cleveland State University, d.munther@csuohio.edu

Mojtaba Sharifi
University of Alberta

Patricio A. Vela
School of Electrical and Computer Engineering

Enhancing produce safety: State estimation-based robust adaptive control of a produce wash system

Vahid Azimi Daniel Munther Mojtaba Sharifi Patricio A. Vela

ARTICLE INFO

Keywords:
Produce wash system
Robust adaptive sliding mode control
Pathogen levels
Hybrid extended Kalman filter

ABSTRACT

The rapid introduction of fresh-cut produce into a produce wash system can dramatically decrease the free chlorine (FC) concentration level in the wash water, resulting in potential widespread cross-contamination throughout the entire wash system. To minimize such contamination, a sufficient level of FC must be maintained in the wash water. This paper presents a state estimation-based robust adaptive sliding mode (RASM) control strategy for the wash system to stabilize the FC concentration level during fresh-cut iceberg lettuce washing. This feedback control law for FC dosing is suggested to provide a sufficient FC injection rate (FCIR) to the wash system in order to compensate for the fall in the FC level and in turn to minimize the *Escherichia coli (E. coli) O157:H7* levels on washed lettuce and in the wash water. The proposed controller uses the estimated chemical oxygen demand (COD) and FC concentration as feedback signals while system states are estimated by a hybrid extended Kalman filter (HEKF) and the unknown noise statistics are identified by a noise identification (NI) algorithm. Uniformly ultimately boundedness (UUB) of the FC concentration tracking error in the presence of unmodelled dynamics is proven using the Lyapunov framework and Barbalat's lemma. The *E. coli O157:H7* contamination levels are predicted from the joint estimator and controller properties. Simulation results show that the proposed NI-based HEKF/RASM control methodology achieves FC tracking while the pathogens converge to their predicted levels. The *E. coli O157:H7* levels decrease as FC concentration increases and in particular, no *E. coli O157:H7* is detected when FC concentration is regulated at 15 mg/L. Two robustness tests are performed to show the performance of the proposed controller in the presence of chlorine actuator failure and system parameter uncertainties. Finally, cross-contamination management is examined in terms of the prevalence and mean pathogen levels of incoming pre-wash lettuce in the context of FC regulation at 15 mg/L.

1. Introduction

Pathogen contamination associated with fresh-cut produce has been linked to numerous food-borne illness outbreaks [1–3]. From the 2006 North American *E. coli* O157:H7 spinach outbreak to the recent (winter 2018) outbreaks associated to romaine lettuce, these illnesses continue to impose heavy burdens on public health [4]. While "best practices" have been developed and continue to improve for multiple stages of the supply chain, ranging from on the farm strategies to processing, transport and storage procedures, given the increasing complexity of the fresh-produce supply chain and the increased demand for fresh products, more insight is needed. For instance, washing and sanitization is a crucial step to ensure fresh produce safety. However, maintaining adequate sanitizer levels in produce wash water during high speed industrial processing is still a technical challenge. Not meeting this need is problematic as significant variations in sanitizer concentrations may give rise to conditions that are favorable for bacterial cross-contamination during washing, thus increasing the potential for produce related outbreaks.

To address the disinfection problem, pathogen level regulation is connected to chlorine concentration regulation. Doing so for a produce wash system model with model uncertainty and discrete measurement times involves a state estimation-based robust

Abbreviations: COD, chemical oxygen demand; FC, free chlorine; FCIR, FC injection rate; *E. coli*, *Escherichia coli*; MPN, most probable number; RASM, robust adaptive sliding mode; HEKF, hybrid extended Kalman filter; NI, noise identification; PSO, particle swarm optimization; RMSE, root mean square error; UUB, uniformly ultimately boundedness.

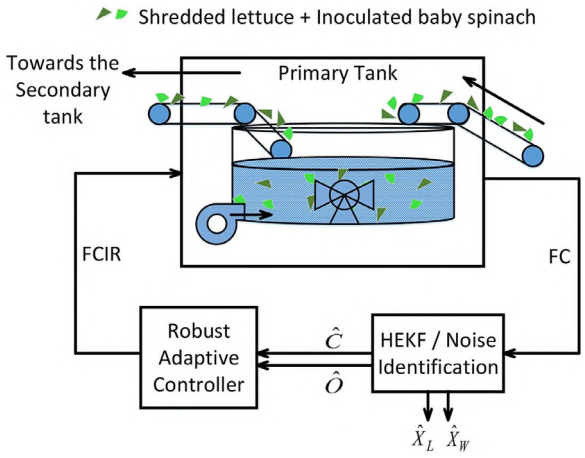

Fig. 1. Proposed structure for the HEKF-based robust adaptive sliding mode controller.

adaptive controller whose objective is to stabilize the free chlorine (FC) concentration to a target level. Achieving the target FC concentration in the wash water minimizes microbial risks and pathogen contamination during the wash process. The paper's objective is to guarantee convergence/boundedness of the FC concentration tracking error in the presence of modeling error and disturbances. The proposed controller is implemented on a simulated, pilot-scale double wash commercial system. Simulations show that the proposed controller effectively meets performance requirements such as state estimation, tracking, and robustness to unmodelled dynamics and disturbances. Further analysis provides insights into the closed-loop pathogen concentration dynamics.

1.1. Background

In recent years, numerous studies have examined fresh-cut produce washing to address how the microbial risks and pathogen contamination can be decreased during the washing process [5–12]. Experiments show that rapid input of fresh-cut produce into the wash system, shown in Fig. 1, decreases the FC level, promoting the potential for wash water induced pathogen cross-contamination [13–15]. Under this situation, an appropriate FC injection rate (FCIR) into the wash tank compensates for the drop in the FC level and in turn reduces the risk of cross-contamination via water [16–18]. Chlorine is a conventional sanitizer used in the fresh-cut produce industry [19,20]. However, maintaining a constant level of the FC concentration during the washing process is a challenging task because of the continuous and rapid introduction of organic material into the wash water.

Given these dynamics, it is crucial to know what amount of FC concentration is required to keep wash water and fresh-cut produce "free" from human pathogens, that is to keep pathogen counts below detection levels. Experiments reveal that higher FC concentration results in lower pathogen levels during washing [21]. Although the U.S. Food and Drug Administration recommends up to 200 mg/L FC concentration during washing, most commercial wash systems maintain a minimum level of FC to inactivate the *E. coli O157:H7* and simultaneously reduce the production of harmful byproducts during processing [21,22]. In [22], a minimum level of FC was prescribed to inactivate *E. coli O157:H7* in industrial wash water during fresh-cut processing. In [21], a comprehensive experiment was carried out and a sufficient FC concentration was suggested for preventing pathogen cross-contamination during washing operations for fresh-cut produce. That work has reported that no cross contamination is observed when the FC concentration was maintained at level greater than or equal to 10 mg/L. In addition to that, in [23], a comprehensive study was performed on the significance of regulating sufficient FC concentration to eliminate bacterial survival. That work showed that a concentration of at least 10 mg/L FC in the wash water is needed to significantly reduce the cross contamination of the washed produce. When the FC concentration was maintained below 10 mg/L, the produce was contaminated. Whereas, for a FC concentration above 10 mg/L, very few samples were found, and in particular, above 20 mg/L, no survival was observed.

1.2. Motivation and contribution

Due to the fact that a mathematical model is an approximated version of an actual system, modeling errors are inevitable. However, robust controllers can mitigate the effects of such modeling errors on system performance and stability [24–26]. The sliding mode control approach is a widely applied robust controller that handles uncertain nonlinear systems and ensures the stability of a closed-loop system [27,28]. Several results of sliding mode controllers have recently been applied in various areas such as agriculture irrigation [29], chemical processes [30,31], and fuel cells [32]. Adaptive control implements learning and adaptation using online parameter estimation for managing system uncertainties. Adaptive components enhance the performance of robust controllers [33–36].

For produce wash systems, the existence of unmodeled dynamics, such as water recirculation dynamics [37] and chlorine breakpoint phenomena [38], may degrade the closed-loop performance or even lead to instability. In addition, when abnormal operations occur in chlorine actuators, regulation of the FC is negatively impacted. More importantly, real-time water quality measurements (such as COD and even FC) with respect to product specific washing specifications may not be available. Even if such data can be consitently obtained, it is not immediately apparent how the measurements can support the target outcomes through feedback control. Motivated by the aforementioned issues and the challenge of maintaining a stable FC level during the wash process, this paper employs model-based robust adaptive control for regulating a produce wash system. It also provides an accompanying analysis of the controller's parametric sensitivity relative to target outcomes (chlorine and pathogen concentrations). The analysis informs deployment options for meeting the outcomes under modeling uncertainty.

In our prior work [38], a noise identication-based hybrid extended Kalman filter (NI-based HEKF) was designed for a produce wash system to estimate the states of the system while only discrete-time measurements of the FC were available. However, in that paper, (i) the FCIR to the wash tank was manually chosen; (ii) there was no feedback control to stabilize the FC concentration and in turn to minimize the pathogen levels; and (iii) a prediction of *E. coli O157:H7* levels relative to a specific level of FC concentration was not established. However, this present paper adds the following original contributions: (a) formulating a robust adaptive sliding mode (RASM) controller to stabilize the FC concentration level and to minimize the *E. coli O157:H7* levels while using the estimated states from the NI-based HEKF algorithm, (b) proving boundedness of the FC concentration tracking error in the presence of unmodeled dynamics and estimation error, (c) predicting the pathogen levels from the target FC level, tracking and estimation bounds, and the average pre-wash pathogen counts on produce, (d) evaluating the controller's robustness to chlorine actuator failures and system parameter uncertainties, and (e) quantifying the effects of pathogen-to-water shedding rate on pathogen levels.

In this work, the RASM controller is first formulated to regulate the FC concentration to the targeted level. The robust term added to the controller manages unmodeled system dynamics and

disturbances. The robust gain is updated by an adaptation mechanism to compensate for (i) time-varying disturbances stemming from possible actuator failure, and (ii) estimation error variations due to system parameter uncertainties and neglected dynamics. The adaptation mechanism uses a dead-zone modification to prevent unfavorable robust gain drift, and to trade off FCIR chattering and FC concentration tracking accuracy. Unlike baseline robust controllers with constant gains, our method renders better control optimality and stronger robustness in the presence of unexpected actuator failures. The proposed controller uses the estimated COD and FC concentration, which are estimated by the HEKF while the unknown noise statistics of the wash system are identified by the NI algorithm. Stability analysis is carried out in the presence of the unmodeled dynamics, system parameter uncertainty, and the estimation error. Boundedness of the actual FC concentration to a compact ball around the target value is proven using the Lyapunov framework and the Barbalat's lemma whose outcomes allow us to predict the pathogen level convergence bounds and limits.

Effectiveness of the proposed controller is evaluated by performing simulation studies on the produce wash system for different target FC concentration levels. Simulation results demonstrate that system states are accurately estimated and the FC concentration is stabilized during the washing process. Results show that the *E. coli O157:H7* levels converge to their predicted values and reduce as the FC level increases. In particular, no *E. coli O157:H7* survives, i.e. pathogens counts are lower than the detection level, when the FC level is regulated at 15 mg/L, which aligns with observations in [21,23]. The proposed structure shows an appropriate robustness in the presence of the parameter uncertainties. Results illustrate that the proposed controller is able to compensate for possible chlorine actuator failure. Results also show that our approach with gain adaptation outperforms the constant-gain controller in the presence of the FC control actuator failures. Finally, the effect of the average pathogen level and prevalence from incoming pre-wash produce is simulated against a FC level regulated at 15 mg/L, providing a quantified link between incoming pathogen levels and the resulting pathogen counts on post-wash produce.

The paper is organized as follows. Section 2 presents the produce wash dynamic model, state estimation algorithm, and the problem statement. Section 3 presents the controller formulation and the pathogen level prediction. Section 4 presents simulation results. Section 5 analyzes effects of pathogen-to-water shedding rate on pathogen levels. Section 6 presents concluding remarks and suggestions for future work.

2. Produce wash dynamic model, state estimation, and problem statement

2.1. Produce wash model description

The evolution equations modeling chlorine and *E. coli* cross-contamination in a commercial wash system (primary tank) [14,37,38] are:

$$\dot{O} = K_0 \tag{1a}$$

$$\dot{C} = -\gamma_c C - \beta_c OC + u \tag{1b}$$

$$\dot{X}_W = \beta_{ws} - \beta_{lw}\left(\frac{L}{V}\right)X_W - \alpha C X_W \tag{1c}$$

$$\dot{X}_L = \beta_{lw}X_W - \alpha C X_L - C_l X_L, \tag{1d}$$

where the non-negative state variables are: O (mg/L) denoting the COD in the wash water, C (mg/L) denoting the FC concentration in the wash water, X_W (MPN/ml) denoting the *E. coli* concentration in the water wash, and X_L (MPN/g) denoting the *E. coli* concentration on the lettuce. Contamination is controlled through u (mg/l min), the control command, which is the FC injection rate (FCIR) into the wash tank. Key parameters are all positive and include K_0 the COD increase rate, γ_c (1/min) the decay rate of FC in municipal tap water, β_c (L/(mg min)) the second order rate constant describing FC reaction with organics, β_{ws} (MPN/(ml min)) the rate of pathogen entry into the wash water (a function of the pathogen shed rate from produce to water due to shear forces during washing), and β_{lw} (mL/(g min)) the rate of cross-contamination from water to lettuce. Additionally, L (g) is the amount of lettuce in the wash water (assumed to be constant, on average), V (mL) is the volume of the wash tank, α (L/(mg min)) is the killing rate due to FC, and $1/C_l$ is the average dwell time of the lettuce in the wash tank (C_l is the reciprocal of the average wash time). The full system state vector is $x = [O, C, X_W, X_L]^T$. The system parameters are the general vector $\Theta = [K_0, \gamma_c, \beta_c, \beta_{ws}, \beta_{lw}, L, V, \alpha, C_l] \in \Re^9$.

Several additional details of the process include the assumption that the pH is regulated to be 6.5 during the wash process. The model described in Eq. (1) involves FC control for disinfection with pH tightly regulated. In addition, the wash model simulation properties include (i) a fixed time wash process for introduced produce lasting 36 min during which the incoming produce rate is fixed, (ii) the tank water volume is constant with recirculating wash water, (iii) contaminated spinach acts as the pathogen delivery vehicle to the wash water (i.e., the spinach and lettuce had no contact until both were put into the water) [21,37]. The equations in (1) model the washing of spinach and fresh cut lettuce together, where the cross-contamination dynamic only considers pathogen transfer from spinach to water to lettuce and ignores direct contact transmission between spinach and lettuce. Therefore, X_L reflects the pathogen level on the lettuce in the wash tank due to cross-contamination from wash water.

2.2. State estimation using HEKF and noise identification algorithm

Mitigation of pathogen levels requires maintaining sufficient FC levels in the face of the introduction of large amounts of organic material from washed produce. For this purpose, the feedback control signal will require the COD and FC concentration state coordinates. Since real-time measurements of these variables may not be possible, this paper uses an HEKF algorithm to estimate the produce wash states with the FC being the only measured quantity. The "hybrid" adjective refers to the discrete-time availability of the FC concentration measurements versus the continuous-time model of the commercial wash process.

Generically, the continuous produce wash system of Eq. (1) with discrete measurements follows

$$\dot{x} = f(x, u, \Theta, w_s(t), t) \text{ with } w_s(t) \sim (0, Q_s) \tag{2a}$$

$$y_k = h_k(x_k, v_{s_k}) \text{ with } v_{s_k} \sim (0, R_{s_k}) \tag{2b}$$

for discrete time points indexed by k, where $f(.)$ represents the process dynamics and $h_k(.)$ is the measurement equations, with $y_k \in \Re$ as the discrete-time FC measurement. The variable $w_s(t) \in \Re^4$ stands for continuous-time white process noise vector with covariance $Q_s \in \Re^{4\times 4}$ and $v_{s_k} \in \Re$ represents discrete-time white measurement noise with covariance $R_{s_k} \in \Re$. The filter estimates are initialized to be

$$\hat{x}_0^+ = \mathrm{E}[x_0], \text{ and}$$
$$P_0^+ = \mathrm{E}\left[(x_0 - \hat{x}_0^+)(x_0 - \hat{x}_0^+)^T\right], \tag{3}$$

where E[.] stands for the expected value operation; P_0^+ is the covariance of the initial estimate; and x_0 and $\hat{x}_0^+$ are the initial values of the state and its estimate.

The time-update equations for states and covariance are given as [38,39]

$$\dot{\hat{x}} = f(\hat{x}, u, \hat{\Theta}, 0, t),$$
$$\dot{P} = AP + PA^T + LQ_f L^T, \tag{4}$$

where A and L are the partial derivatives of f w.r.t. x and w_s evaluated at the current estimated state; and Q_f denotes the filter process noise covariance. At each measurement time, the state estimate and the covariance are updated as

$$K_k = P_k^- H_k^T \left(H_k P_k^- H_k^T + M_k R_{f_k} M_k^T\right)^{-1},$$
$$\hat{x}_k^+ = \hat{x}_k^- + K_k\left(y_k - h_k(\hat{x}_k^-, 0, t_k)\right),$$
$$P_k^+ = (I - K_k H_k) P_k^- (I - K_k H_k)^T + K_k M_k R_{f_k} M_k^T K_k^T, \tag{5}$$

where H_k and M_k are the partial derivatives of h_k w.r.t. x_k and v_{s_k} evaluated at the current predicted state; K_k is the Kalman filter gain; and R_{f_k} denotes the filter measurement noise covariance.

Remark 1. The process and measurement noise covariance matrices of the filter (Q_f, R_{f_k}) are unknown and different than the ones of the system (Q_s, R_{s_k}). The system covariance parameters (Q_s, R_{s_k}) are identified using experimental data per [38].

The HEKF estimation performance depends on the noise relative to the model parameters. As the covariance matrices in the filter (Q_f, R_{f_k}) are unknown, they are calculated by a noise identification algorithm. This algorithm uses a particle swarm optimization (PSO) to optimize the estimator covariance matrices for estimation performance.

Assumption 1. The process and measurement noises are uncorrelated.

According to Assumption 1, the problem is to estimate the four diagonal elements of Q_f and the single element of R_{s_k} to achieve an optimal state estimation, that is the innovations $y_k - h_k\hat{x}^-$ are (i) white noise with (ii) zero mean and with (iii) covariance of $H_k R_k^- H_k^T + Rs_k$. The joint HEKF and the noise identification algorithm leads to an NI-based HEKF algorithm to estimate the system states and unknown noise statistics [38].

Property 1. *The norm of the estimation error is bounded by a positive scalar $\|e_e\| \leq \epsilon_e$. Consequently, the FC concentration and COD estimation errors, denoted by $\hat{e}_C$ and $\hat{e}_O$, respectively, are bounded, e.g., $|\hat{e}_C| \leq \epsilon_C$ and $|\hat{e}_O| \leq \epsilon_O$ by positive scalars ϵ_C and ϵ_O.*

Convergence of the estimator to the true states cannot be guaranteed, however boundedness of the estimation error of the EKF is guaranteed using stochastic Lyapunov functions if the initial estimation error $e_e(0)$, control input u, and disturbances are bounded [40,41]. Thus, Property 1 reflects bounded error operation of the NI-based HEKF arising from bounded error initial conditions and bounded disturbances. This outcome is exploited in the robust controller.

2.3. Problem statement

Organic matter entering the wash tank lowers the FC level (as determined by the rate constant β_c) thereby increasing the risk of cross-contamination [13,14]. Injecting more FC into the primary wash tank counters this effect. To prevent overchlorination of the wash water, the FC concentration should be regulated by managing the FCIR. This paper details a RASM control strategy for the produce wash system that stabilizes the FC concentration to a target level and is robust to uncertainty in the model dynamics. Given a fixed input rate of *E. coli* shed into the wash water from contaminated produce (β_{ws}), the resulting pathogen levels transferred to the water and the lettuce are predicted based on the prescribed FC concentration level in the water tank. The proposed controller uses the COD and FC concentrations, estimated by the NI-HEKF algorithm, as feedback signals. A joint robust component and adaptation mechanism promote system robustness to unmodeled dynamics, estimation error, and disturbances. The boundedness of the FC concentration tracking error to a compact set around the desired value is proved using the Lyapunov framework and the Barbalat's lemma. The proposed estimation-based control approach is finally implemented on the produce wash system illustrated in Fig. 1.

3. Proposed controller for the wash system

Regulating the FC concentration involves focusing on the equation Eq. (1b) while modeling the effects due to the other variables as external disturbances. For example, water is recirculated to the tank during the wash process [37]. Due to the lack of a model for the quantity of COD and free chlorine returning to the tank, the recirculation dynamic is neglected. Additionally, the equations do not account for chlorine breakpoint phenomena [38]. Both of these unmodeled effects are considered by the unknown function $f_{un}(C, O)$ in the chlorine update equations. Lastly, FC actuation failures may lead to free chlorine concentration changes that differ from those intended. These will be described by $u_d(t)$, but with the time argument removed in displayed equations, generically representing an unknown actuator disturbance. Together, these contributions lead to the free chlorine dynamics,

$$\dot{C} = -\gamma_c C - \beta_c OC - f_{un}(C, O) + u + u_d. \tag{6}$$

Replacing the C dependent dynamics with a linearly parametrized regressor, they become

$$\dot{C} = -Y(C, O)\theta - f_{un}(C, O) + u + u_d, \tag{7}$$

where $Y(C, O) = [C, OC] \in \Re^{1\times r}$ with $r = 2$ is the model regressor matrix and $\theta = [\gamma_c, \beta_c]^T \in \Re^{r\times 1}$ is the unknown parameter vector.

These equations will be the core equations for deriving a control law u with the objective of regulating the FC concentration to meet a desired minimum level. The estimated COD ($\hat{O}$) and FC concentration ($\hat{C}$) will be used as feedback signals for the controller.

Abnormal operation for the actuator leads to a reduced or increased FCIR relative to the desired rate. It is modeled by the disturbance $u_d(t)$ to the system. During abnormal operation the demanded control signal cannot be effected and will negatively impact regulation of the FC concentration. Under total failure, nothing can be done as it is the only control signal available. For tractable analysis, we will assume that actuator failure can only be partial, implying a bounded error in the target FCIR.

Assumption 2 Partial actuator failure. The time-varying disturbance $u_d(t)$ occurs for a small time duration $T > 0$ and is uniformly bounded by $|u_d(t)| \leq \bar{u}_d$, for $\bar{u}_d > 0$.

3.1. Robust adaptive sliding mode (RASM) controller

To regulate the system in the face of parameter uncertainties, neglected dynamics $f_{un}(O, C)$, actuation disturbances $u_d(t)$, and state estimation error, all of which degrade the performance of the closed-loop system, a RASM will be applied. Given system parameters estimate $\hat{\theta}$ and the state signal estimates, the RASM controller is:

$$u = \dot{C}^d + \hat{\gamma}_c\hat{C} + \hat{\beta}_c\hat{O}\hat{C} - \lambda\hat{e} - k_d \text{sat}\left(\frac{\hat{e}}{\phi}\right) = \dot{C}^d + Y(\hat{C}, \hat{O})\hat{\theta}$$
$$- \lambda\hat{e} - k_d(t)\text{sat}\left(\frac{\hat{e}}{\phi}\right), \tag{8}$$

where C^d is the desired FC concentration so that $\dot{C}^d$ is a feedforward term for the desired rate of change of C; $Y(\hat{C}, \hat{O}) = [\hat{C}, \hat{O}\hat{C}]$

is the estimated model regressor matrix for canceling the associated system dynamics; λ is a positive scaling factor of the estimated tracking error $\hat{e} = \hat{C} - C^d$ for aiding in stabilization; and $k_d(t)$ is the time-varying control gain for the robust term compensating for unmodeled dynamics and disturbance. The regression parameter vector $\hat{\theta} = [\hat{y}_C, \hat{\beta}_C]^T$ represents the estimates of θ such that $\hat{\theta} = \theta + \tilde{\theta}$, with $\tilde{\theta}$ being the parameter estimate deviation from its nominal value. The function sat(.) denotes the saturation function, defined as:

$$\text{sat}\left(\frac{\hat{e}}{\phi}\right) = \begin{cases} \frac{\hat{e}}{\phi} & \text{if } |\hat{e}| \le \phi \\ -1 & \text{if } \hat{e} < -\phi \\ +1 & \text{if } \hat{e} > +\phi \end{cases}, \tag{9}$$

where ϕ is width of the saturation function.

To relieve the engineer of the need to manually tune the gain k_d in the presence of neglected dynamics $f_{un}(C, O)$, disturbance $u_d(t)$, and state estimation error e_e, the following adaptation law will update the gain

$$\dot{k}_d = k_{d_0} |\hat{e}_\Delta| \tag{10}$$

with positive scalar k_{d_0} and dead-zone modification as [26,42]

$$\hat{e}_\Delta = \begin{cases} \hat{e} - \phi \text{sat}(\frac{\hat{e}}{\phi}) & \text{if } |\hat{e}| > \phi \\ 0 & |\hat{e}| \le \phi \end{cases}. \tag{11}$$

The reason for having the control law of Eq. (8) in conjunction with the gain update law of Eq. (10) is three-fold [47]: (i) the adaptation law tunes $k_d(t)$ for sufficiently large tracking error ($|\hat{e}| > \phi$) and stops tuning when the error trajectory lies in the dead-zone region ($-\phi \le \hat{e} \le \phi$). Small tracking errors are usually caused by the measurement noise, to which the adaptation mechanism should be insensitive; (ii) the controller trades off between FCIR chattering and FC concentration tracking performance; and (iii) the controller bounds the gain evolution and the error trajectory in the boundary layer $|\tilde{e}| \le \phi$, leading to UUB of all system solutions.

Writing the true tracking error as a function of the FC estimation error $\hat{e}_C = \hat{C} - C$, C, and C^d gives

$$\hat{e} = C + \hat{e}_C - C^d \tag{12}$$

whose time derivative along with the system in Eq. (6) is

$$\dot{\hat{e}} = \dot{C} + \dot{\hat{e}}_C - \dot{C}^d = -Y(C, O)\theta - f_{un}(C, O) + u + u_d + \dot{\hat{e}}_C - \dot{C}^d. \tag{13}$$

Further substitution of the controller from Eq. (8) gives

$$\begin{aligned} \dot{\hat{e}} &= -Y(C, O)\theta - f_{un}(C, O) + \dot{C}^d - \lambda\hat{e} \\ &\quad + Y(\hat{C}, \hat{O})\hat{\theta} - k_d(t)\text{sat}\left(\frac{\hat{e}}{\phi}\right) + u_d + \dot{\hat{e}}_C - \dot{C}^d \\ &= -\lambda\hat{e} - k_d(t)\text{sat}\left(\frac{\hat{e}}{\phi}\right) + Y(\hat{C}, \hat{O})\hat{\theta} \\ &\quad - Y(C, O)\theta - f_{un}(C, O) + u_d + \dot{\hat{e}}_C \end{aligned} \tag{14}$$

Define the regressor error $e_Y = Y(\hat{C}, \hat{O}) - Y(C, O)$ to emphasize the effects of estimation errors on the error dynamics,

$$\dot{\hat{e}} = -\lambda\hat{e} - k_d(t)\text{sat}\left(\frac{\hat{e}}{\phi}\right) + e_Y\hat{\theta} + Y(C, O)\tilde{\theta} - f_{un}(C, O) + u_d + \dot{\hat{e}}_C. \tag{15}$$

To provide context for the mismatch terms contained in Eq. (15), their roles and properties are described below. In particular, manipulations and consideration of physical constraints on the process dynamics leads to linear plus bounded defect inequality bounds on the absolute values of these mismatch terms.

3.1.1. Term $f_{un}(C, O)$

The unmodeled dynamics $f_{un}(C, O)$ are structurally unknown but must satisfy certain properties based on physical considerations. Since this contribution models uncertain recirculation and breakpoint dynamics such that it is impossible to recirculate or to break down more chemical concentration than exists in the water, these functions are necessarily limited in terms of the potential function classes they can belong to. We first make an assumption on $f_{un}(C, O)$ that covers a wide variety of physically motivated unmodeled dynamics.

Assumption 3. The function f_{un} is a continuous function such that there exists a constant b_1 and a bounded function $\tilde{f}_{un}(C, O)$ for which the unmodeled dynamics $f_{un}(C, O)$ have a linear in C contribution plus a bounded or saturated in C and O contribution $\tilde{f}_{un_2}$ as

$$f_{un}(C, O) = b_1 C + \tilde{f}_{un}(C, O). \tag{16}$$

While $f_{un}(C, O)$ may depend linearly or non-trivially on O, the nature of the COD dynamics (1a) (which tend to increase linearly in the wash water relative to the produce input rate) and the fixed time duration of the wash process implies that the COD lies in a compact domain with upper bound

$$O_0 \le O \le K_0 t_f + O_0 = \bar{O}, \tag{17}$$

where O_0 is the initial value of O and t_f is the final time (here 36 min). Thus dependence on O is necessarily bounded by a linear function of C plus a constant value in the worst case. Combining the simplified form of the unmodeled dynamics for C and O together leads to a function of the form of Eq. (16). With C being unknown but satisfying $C = \hat{e} - \hat{e}_C + C^d$ means that we can define an alternative function form for f_{un} in terms of these other variables,

$$f_{un}(\hat{e}, \hat{e}_C, C^d, O, t) = b_1\hat{e} + \tilde{f}_{un}(\hat{e}_C, C^d, O), \tag{18}$$

where we likewise exploit the known boundedness of $\hat{e}_C$ and C^d. Using the boundedness of $\tilde{f}_{un}$ to define the upper bound $|\tilde{f}_{un}| \le D_1(\epsilon_C, \bar{O}, C^d)$, implies that

$$|f_{un}(\hat{e}, \hat{e}_C, C^d, O, t)| \le |b_1||\hat{e}| + D_1 = B_1 E, \tag{19}$$

where $B_1 = [\bar{b}_1, D_1]$, $E = [|\hat{e}|, 1]^T$, and $|b_1| \le \bar{b}_1$.

Remark 2. Eq. (16) suggests a model for the neglected dynamics in Eq. (1b) that is motivated by physical characteristics involved in produce washing. For instance, the first term of this equation ($b_1 C$) gives a simple account of the typical practice of water recirculation to the tank during the wash process and the second term ($\tilde{f}_{un}$) treats chlorine breakpoint phenomena which involves nonlinear but bounded dynamics (since washing operates on a finite time scale).

3.1.2. Term $e_Y\hat{\theta}$

Manipulating $e_Y\hat{\theta}$, we have

$$\begin{aligned} e_Y\hat{\theta} &= \left(Y(\hat{C}, \hat{O}) - Y(C, O)\right)\hat{\theta} \\ &= \left(\begin{bmatrix} \hat{C} \\ \hat{O}\hat{C} \end{bmatrix} - \begin{bmatrix} C \\ OC \end{bmatrix}\right)^T \hat{\theta} = \begin{bmatrix} \hat{e}_C \\ \hat{O}\hat{C} - OC \end{bmatrix}^T \hat{\theta}. \end{aligned} \tag{20}$$

Use $\hat{O} = O + \hat{e}_O$, $\hat{C} = C + \hat{e}_C$, and $C = \hat{e} - \hat{e}_C + C^d$ to rewrite Eq. (20)

$$e_Y\hat{\theta} = \begin{bmatrix} \hat{e}_C \\ \hat{e}_O\hat{e} + \hat{e}_O C^d + \hat{e}_C O \end{bmatrix}^T \hat{\theta} = \hat{e}_O \begin{bmatrix} 0 \\ \hat{e} \end{bmatrix}^T \hat{\theta} + \begin{bmatrix} \hat{e}_C \\ \hat{e}_O C^d + \hat{e}_C O \end{bmatrix}^T \hat{\theta}. \tag{21}$$

Recall that the parameter estimate $\hat{\theta}$ is bounded and due to Property 1 the estimation errors $\hat{e}_O$ and $\hat{e}_C$ are also bounded. In conjunction with Eq. (17), these bounds mean that $|e_Y\hat{\theta}|$

is bounded by a linear function of $|\hat{e}|$ plus a bounded term $D_2(\epsilon_C, \epsilon_O, \bar{O}, C^d, \hat{\theta}) \geq 0$ such that

$$|e_Y\hat{\theta}| \leq |b_2||\hat{e}| + D_2 = B_2E, \tag{22}$$

where $B_2 = [\bar{b}_2, D_2]$, $b_2 = \hat{e}_O\hat{\theta}_2$, and $|b_2| \leq \bar{b}_2 = \epsilon_O\hat{\theta}_2$.

3.1.3. Term $Y(C,O)\tilde{\theta}$

Using $C = \hat{e} - \hat{e}_C + C^d$, the term $Y(C,O)\tilde{\theta}$ has the alternative form

$$Y(C,O)\tilde{\theta} = \begin{bmatrix} C \\ OC \end{bmatrix}^T \tilde{\theta} = \begin{bmatrix} 1 \\ O \end{bmatrix}^T \tilde{\theta}\hat{e} + \begin{bmatrix} 1 \\ O \end{bmatrix}^T \tilde{\theta}(C^d - \hat{e}_C). \tag{23}$$

Boundedness of $\hat{e}_C$, O, and $\tilde{\theta}$, means that $|Y(C,O)\tilde{\theta}|$ is bounded by linear in $|\hat{e}|$ and bounded terms,

$$|Y(C,O)\tilde{\theta}| \leq |b_3||\hat{e}| + D_3 = B_3E, \tag{24}$$

where $B_3 = [\bar{b}_3, D_3]$, $b_3 = \tilde{\theta}_1 + O\tilde{\theta}_2$, $|b_3| \leq \bar{b}_3 = |\tilde{\theta}_1| + \bar{O}|\tilde{\theta}_2|$, and the bounded term is $D_3(\bar{O}, \epsilon_C, \|\tilde{\theta}\|) \geq 0$.

3.1.4. Term $\dot{\hat{e}}_C$

The derivative of the FC estimation error is

$$\begin{aligned} \dot{\hat{e}}_C = \dot{\hat{C}} - \dot{C} &= -Y(\hat{C},\hat{O})\hat{\theta} + u + Y(C,O)\theta + f_{un}(C,O) - u - u_d \\ &= Y\tilde{\theta} - e_Y\hat{\theta} + f_{un}(C,O) - u_d \end{aligned} \tag{25}$$

for which the bounds for the constitutive terms were just detailed. The bound for $|\dot{\hat{e}}_C|$ is obtained as

$$|\dot{\hat{e}}_C| \leq |f_{un}(C,O)| + |e_Y\hat{\theta}| + |Y\tilde{\theta}| + |u_d| = (B_1 + B_2 + B_3)E + \bar{u}_d \tag{26}$$

Simplifying these uncertain terms to linear in $\hat{e}$ plus bounded or saturating terms admits more explicit analysis of the Lyapunov rate bounds for the closed-loop subsystem of the wash process. Whereby, using the previously computed bounds,

$$|f_{un}| + |e_Y\hat{\theta}| + |Y\tilde{\theta}| + |\dot{\hat{e}}_C| + |u_d| \leq \bar{b}|\hat{e}| + D \tag{27}$$

with $\bar{b} = 2\left(\bar{b}_1 + \bar{b}_2 + \bar{b}_3\right)$ and $D = 2(\bar{u}_d + D_1 + D_2 + D_3)$.

3.2. Stability analysis

Using the control and adaptation laws of Eqs. (8) and (10), the FC tracking error and the gain remain bounded for all time. The following Lyapunov function shows the boundedness of all system solutions,

$$V(\hat{e}_\Delta, \tilde{k}_d) = \frac{1}{2}\hat{e}_\Delta^2 + \frac{1}{2k_{d_0}}\tilde{k}_d^2, \tag{28}$$

where $\tilde{k}_d = k_d - \bar{k}_d$ such that $\bar{k}_d$ is the positive ideal gain.

Barbalat's lemma [43] is a useful tool in stability analysis of nonlinear systems and also used to verify the asymptotic convergence of adaptive control systems. A version of it can be stated as follows:

Lemma 1 Barbalat's Lemma. *If a function $g(t)$ is uniformly continuous[1] for all $t \geq 0$ and if the limit of the integral $\lim_{t\to\infty}\int_0^t g(h)dh$ exists and is finite, then $\lim_{t\to\infty} g(t) = 0$.*

Theorem 1. *Consider the FC error dynamics of es (13), the FC dosing control law of Eq. (8), and the adaptation law of Eq. (10). Under Property 1, and Assumptions 1, 2, and 3, the uniform ultimate boundedness[2] of all system solutions $(\hat{e}, k_d)$ is guaranteed for unknown $\Theta \in \Re^9$, u_d, and f_{un}, and any $\hat{e}(0) \in \Re$, when $\lambda > \bar{b}$.*

Proof of Theorem 1. The proof relies on the Lyapunov function of Eq. (28). First consider $|\hat{e}| > \phi$, for which $\dot{\hat{e}}_\Delta = \dot{\hat{e}}$. Substituting Eq. (15) into the derivative of Eq. (28) yields

$$\begin{aligned} \dot{V} = &-\hat{e}_\Delta\lambda\hat{e} - \hat{e}_\Delta k_d \mathrm{sat}(\frac{\hat{e}}{\phi}) - \hat{e}_\Delta f_{un}(C,O) + \hat{e}_\Delta u_d(t) \\ &+ \hat{e}_\Delta\dot{\hat{e}}_c + \hat{e}_\Delta e_Y\hat{\theta} + \hat{e}_\Delta Y\tilde{\theta} + \frac{1}{k_{d_0}}\dot{k}_d(k_d - \bar{k}_d). \end{aligned} \tag{29}$$

Substitute Eq. (10) into Eq. (29), then use the definition of $\hat{e}_\Delta$ and the property $\mathrm{sat}(\frac{\hat{e}}{\phi})\hat{e}_\Delta = |\hat{e}_\Delta|$, to obtain

$$\begin{aligned} \dot{V} = &-\lambda\hat{e}_\Delta^2 - |\hat{e}_\Delta|\lambda\phi - |\hat{e}_\Delta|k_d - \hat{e}_\Delta f_{un}(C,O) + \hat{e}_\Delta u_d(t) \\ &+ \hat{e}_\Delta\dot{\hat{e}}_c + \hat{e}_\Delta e_Y\hat{\theta} + \hat{e}_\Delta Y\tilde{\theta} + |\hat{e}_\Delta|k_d - |\hat{e}_\Delta|\bar{k}_d \end{aligned} \tag{30}$$

that can be simplified as

$$\begin{aligned} \dot{V} \leq &-\lambda\hat{e}_\Delta^2 - |\hat{e}_\Delta|\lambda\phi + |\hat{e}_\Delta||f_{un}(C,O)| + |\hat{e}_\Delta||u_d(t)| \\ &+ |\hat{e}_\Delta||\dot{\hat{e}}_c| + |\hat{e}_\Delta||e_Y\hat{\theta}| + |\hat{e}_\Delta||Y\tilde{\theta}| - |\hat{e}_\Delta|\bar{k}_d. \end{aligned} \tag{31}$$

Substitute the calculated bounds from Section 3.1 to yield

$$\dot{V} \leq -\lambda\hat{e}_\Delta^2 + 2|\hat{e}_\Delta|(B_1 + B_2 + B_3)E + 2|\hat{e}_\Delta|\bar{u}_d - |\hat{e}_\Delta|(\bar{k}_d + \lambda\phi), \tag{32}$$

which can be written as

$$\begin{aligned} \dot{V} \leq &-\lambda\hat{e}_\Delta^2 + 2|\hat{e}_\Delta|(\bar{b}_1 + \bar{b}_2 + \bar{b}_3)|\hat{e}| + |\hat{e}_\Delta|(2(D_1 + D_2 + D_3 + \bar{u}_d) \\ &- (\bar{k}_d + \lambda\phi)). \end{aligned} \tag{33}$$

Use the definition of $\hat{e} = \hat{e}_\Delta + \phi\mathrm{sat}(\frac{\hat{e}}{\phi})$ for $|\hat{e}| > \phi$, and the definitions of D and $\bar{b}$, to obtain

$$\dot{V} \leq -(\lambda - \bar{b})\hat{e}_\Delta^2 - \left(\bar{k}_d + (\lambda - \bar{b})\phi - D\right)|\hat{e}_\Delta|. \tag{34}$$

Assume that the ideal gain $\bar{k}_d$ satisfies the following equality condition

$$\bar{k}_d = D + (\bar{b} - \lambda)\phi \tag{35}$$

for which the true knowledge of the ideal gain is not required, only its existence is assumed. Using the equality condition presented in Eq. (35), we then have

$$\dot{V} \leq -(\lambda - \bar{b})\hat{e}_\Delta^2, \tag{36}$$

implying that $\dot{V} \leq 0$ for $\lambda > \bar{b}$.

Let us define $\kappa = \lambda - \bar{b} > 0$ and

$$g(t) = \kappa\hat{e}_\Delta^2, \tag{37}$$

based on which it follows that

$$\dot{V} \leq -g(t). \tag{38}$$

Integrating both sides of Eq. (38) from 0 to ∞ yields

$$V(0) - V(\infty) \geq \lim_{t\to\infty}\int_0^t g(h)dh. \tag{39}$$

Since $\dot{V}(t) \leq 0$, and by definition $V(t) \geq 0$, the left-hand side of Eq. (39) is positive and finite (V is bounded), which follows that the right-hand side of Eq. (39) exists, and is positive and finite. Hence, according to the Barbalat's lemma

$$\lim_{t\to\infty} g(t) = \lim_{t\to\infty} \kappa\hat{e}_\Delta^2 = 0. \tag{40}$$

[1] A function $g(t)$: $\Re \to \Re$ is uniformly continuous on $[0, \infty]$ if $\forall\epsilon > 0$, $\exists\delta(\epsilon) > 0$, $\forall t_1 \geq 0$, $\forall t \geq 0$, $|t - t_1| < \delta \to |g(t) - g(t_1)| < \epsilon$.

[2] The system's solutions $(\hat{e},\ k_d)$ *are uniformly ultimately bounded with ultimate bound b if $\exists b,\ c > 0$ and for every $0 < a < c$, $\exists T > 0$ such that* $\left\|\begin{matrix}\hat{e}(t_0)\\ k_d(t_0)\end{matrix}\right\| \leq a \to \left\|\begin{matrix}\hat{e}(t)\\ k_d(t)\end{matrix}\right\| \leq b,\ \forall t > t_0 + T$.

Since $\kappa > 0$, Eq. (40) implies that $\dot{\hat{e}}_\Delta \to 0$ (i.e., $\dot{\hat{e}} \le \phi$) from which and the boundedness of V it follows that $\bar{k}_d$ is bounded. Going further, since $\bar{k}_d$ is constant, $k_d = \tilde{k}_d + \bar{k}_d$ is bounded. This proves UUB of the system's solutions $(\tilde{e},\ k_d)$.

In case that $|\tilde{e}| > \phi$, the adaptation law presented in Eq. (10) applies to the system until the unmodelled dynamics, disturbances, and estimation error are all compensated for, resulting in the convergence of $\tilde{e}$ to its ultimate bound ϕ. This implies that all error trajectories starting outside the boundary layer will converge to a small neighborhood around the origin, where the size of the neighborhood depends on the selection of the width of saturation function ϕ. Inside the boundary layer ($|\tilde{e}| \le \phi$), $\dot{V}$ can take positive sign. However when $|\tilde{e}| \le \phi$, we have $\tilde{e}_\Delta = 0$ that inactivates the adaptation process, $k_d = 0$. This ensures the boundedness of gain k_d and prevents the potential 'gain drift' phenomenon. Taken altogether, the proposed controller provides the uniformly ultimately boundedness of the system's solutions $(\tilde{e},\ k_d)$ regardless of starting from inside/outside the boundary layer. □

Remark 3. The width of saturation function ϕ trades off between the FC tracking performance and chattering of the FCIR. Although a small value of ϕ provides better tracking, it results in chattering. Adjusting the parameter λ tunes the tracking error convergence rate to achieve better tracking. The rate of convergence depends on the scale of $\bar{b}$ and stability of the system holds when $\lambda > \bar{b}$.

Remark 4. Theorem 1 brings a practical property of the gain selection to light. As shown, if $\lambda > \bar{b}$, the error term has the property that $|\tilde{e}| \le \phi$. Further expanding this condition yields

$$\lambda > 2\Big(\bar{b}_1 + |\tilde{\theta}_1| + \bar{O}|\tilde{\theta}_2| + \epsilon_O\hat{\theta}_2\Big), \tag{41}$$

implying that the choice of the gain λ is dependent on (i) the scale of the constant $\bar{b}_1$ associated with the function f_{un}, (ii) the maximum value of COD, (iii) the COD estimation error, and (iv) the scale of the parameter estimation error.

3.3. Pathogen levels

As the produce wash system has only one control signal (the FC injection rate), only one state can be controlled (in this work, the FC concentration). The other states follow the natural dynamics of Eq. (1), also called the "internal dynamics", and cannot be seen from the input-output $(u - C)$ relationship. However, the purpose of controlling C is to ultimately minimize the internal contamination variables. Section 3.1 formulated a controller to maintain FC concentration within a neighborhood of the desired level C^d. This section shows the convergence of the internal contamination variables X_W and X_L to neighborhoods determined by the neighborhood of C.

Theorem 2. *Given the desired FC concentration level C^d and the proposed Theorem 1, the ultimate bounds for the pathogen levels in the water and on the lettuce are predicted to lie in the intervals determined by the following interval membership equations:*

$$X_W - \bar{X}_W \in [-\delta_W, \delta_W] \quad \text{and} \quad X_L - \bar{X}_L \in [-\delta_L, \delta_L], \tag{42}$$

where

$$\bar{X}_W = \frac{\beta_{ws}\left(\beta_{lw}\frac{L}{V} + \alpha C^d\right)}{\left(\beta_{lw}\frac{L}{V} + \alpha C^d\right)^2 - \alpha^2(\phi + \epsilon_C)^2},$$

$$\delta_W = \frac{\beta_{ws}\alpha(\phi + \epsilon_C)}{\left(\beta_{lw}\frac{L}{V} + \alpha C^d\right)^2 - \alpha^2(\phi + \epsilon_C)^2},$$

$$\bar{X}_L = \frac{\beta_{lw}\bar{X}_W\left(C_l + \alpha C^d\right) + \beta_{lw}\delta_W\alpha\left(\phi + \epsilon_C\right)}{\left(C_l + \alpha C^d\right)^2 - \alpha^2(\phi + \epsilon_C)^2},$$

$$\delta_L = \frac{\beta_{lw}\delta_W\left(C_l + \alpha C^d\right) + \beta_{lw}\bar{X}_W\alpha\left(\phi + \epsilon_C\right)}{\left(C_l + \alpha C^d\right)^2 - \alpha^2(\phi + \epsilon_C)^2} \tag{43}$$

when the estimation and tracking errors are sufficiently small relative to the target concentration C^d ($C^d \gg \phi + \epsilon_C$). For zero-mean estimation and tracking error statistics, the expected pathogen levels match their steady-state values

$$X_{W_{ss}} = \frac{\beta_{ws}}{\left(\beta_{lw}\frac{L}{V} + \alpha C^d\right)} \text{ and } X_{L_{ss}} = \frac{\beta_{lw}\beta_{ws}}{\left(C_l + \alpha C^d\right)\left(\beta_{lw}\frac{L}{V} + \alpha C^d\right)}. \tag{44}$$

Proof of Theorem 2. Since the FC concentration converges to a neighborhood of the target concentration C^d, the equivalent neighborhoods for the *E. coli* concentration in the wash water and on the lettuce can be predicted. Predicting the interval of convergence for X_W requires considering the dynamics in Eq. (1c) while replacing C with $C^d + \tilde{e} - \tilde{e}_C$ (see Eq. (12)) as

$$\dot{X}_W = \beta_{ws} - \left(\beta_{lw}\left(\frac{L}{V}\right) + \alpha\left(C^d + \tilde{e} - \tilde{e}_C\right)\right)X_W. \tag{45}$$

Boundedness of the estimator and controller means that $|\tilde{e}| \le \phi$ and $|\tilde{e}_C| \le \epsilon_C$, which is equivalent to $\tilde{e} \in [-\phi, \phi]$ and $\tilde{e}_C \in [-\epsilon_C, \epsilon_C]$, implying that

$$\begin{aligned}\beta_{ws} - \left(\beta_{lw}\left(\frac{L}{V}\right) + \alpha\left(C^d + \phi + \epsilon_C\right)\right)X_W \le \dot{X}_W \le \beta_{ws}\\ - \left(\beta_{lw}\left(\frac{L}{V}\right) + \alpha\left(C^d - \phi - \epsilon_C\right)\right)X_W.\end{aligned} \tag{46}$$

Employing the Comparison Lemma, the lower and upper bounds for X_W are obtained as

$$\begin{aligned}X_W(t) &\ge \frac{\beta_{ws}}{\left(\beta_{lw}\left(\frac{L}{V}\right) + \alpha\left(C^d + \phi + \epsilon_C\right)\right)} \text{ and}\\ X_W(t) &\le \frac{\beta_{ws}}{\left(\beta_{lw}\left(\frac{L}{V}\right) + \alpha\left(C^d - \phi - \epsilon_C\right)\right)}.\end{aligned} \tag{47}$$

Note that since the FC concentration is a non-negative variable, the term $C = C^d - \phi - \epsilon_C$ is always non-negative. Manipulating both equations to have a common denominator leads to the following re-centered ultimate bound inequality

$$\begin{aligned}&\Big|X_W(t) - \underbrace{\frac{\beta_{ws}\left(\beta_{lw}\frac{L}{V} + \alpha C^d\right)}{\left(\beta_{lw}\frac{L}{V} + \alpha C^d\right)^2 - \alpha^2(\phi + \epsilon_C)^2}}_{\bar{X}_W}\Big|\\ &\le \underbrace{\frac{\beta_{ws}\alpha(\phi + \epsilon_C)}{\left(\beta_{lw}\frac{L}{V} + \alpha C^d\right)^2 - \alpha^2(\phi + \epsilon_C)^2}}_{\delta_W}\end{aligned} \tag{48}$$

For the ultimate bound intervals of X_L, consider the dynamics in Eq. (1d) as

$$\dot{X}_L = \beta_{lw}X_W - \alpha\left(C^d + \tilde{e} - \tilde{e}_C\right)X_L - C_lX_L. \tag{49}$$

Since X_W lies in a ball around $\bar{X}_W$, the following upper and lower inequalities apply to X_L as

$$\begin{aligned}\beta_{lw}\bar{X}_W - \beta_{lw}\delta_W - \left(C_l + \alpha\left(C^d + \phi + \epsilon_C\right)\right)X_L \le \dot{X}_L\\ \le \beta_{lw}\bar{X}_W + \beta_{lw}\delta_W - \left(C_l + \alpha\left(C^d - \phi - \epsilon_C\right)\right)X_L.\end{aligned} \tag{50}$$

Once again employing the Comparison Lemma, the lower and upper bounds are computed as

$$\begin{aligned}X_L(t) &\ge \frac{\left(\beta_{lw}\bar{X}_W - \beta_{lw}\delta_W\right)\left(C_l + \alpha C^d - \alpha\left(\phi + \epsilon_C\right)\right)}{\left(C_l + \alpha C^d\right)^2 - \alpha^2(\phi + \epsilon_C)^2} \text{ and}\\ X_L(t) &\le \frac{\left(\beta_{lw}\bar{X}_W + \beta_{lw}\delta_W\right)\left(C_l + \alpha C^d + \alpha\left(\phi + \epsilon_C\right)\right)}{\left(C_l + \alpha C^d\right)^2 - \alpha^2(\phi + \epsilon_C)^2}.\end{aligned} \tag{51}$$

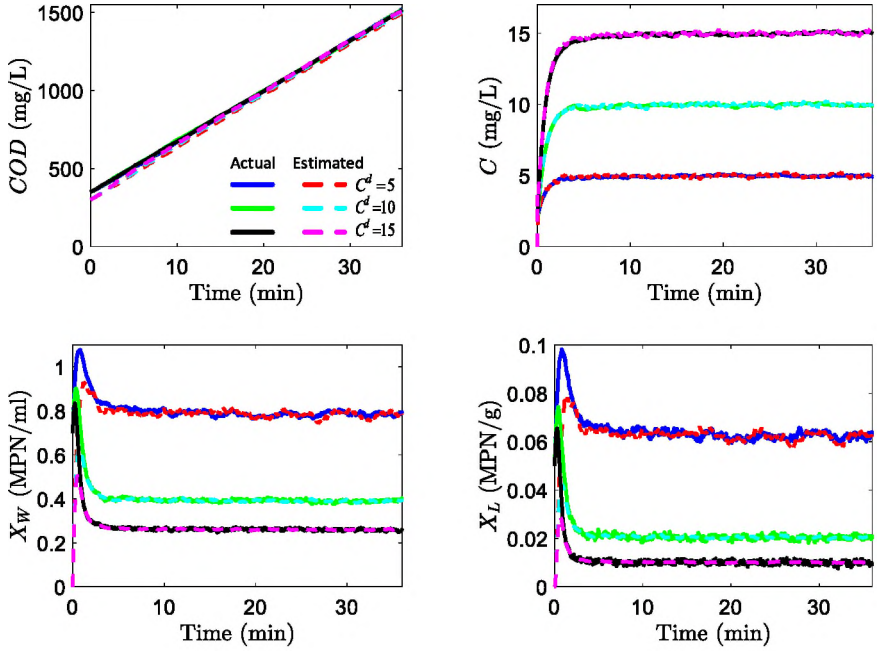

Fig. 2. State estimation performance for different desired FC concentration.

Extracting the common components (added and subtracted) from the two inequalities leads to the following re-centered ultimate bound

$$|X_L(t) - \underbrace{\frac{\beta_{lw}\bar{X}_W\left(C_l+\alpha C^d\right)+\beta_{lw}\delta_W\alpha\left(\phi+\epsilon_C\right)}{\left(C_l+\alpha C^d\right)^2-\alpha^2(\phi+\epsilon_C)^2}}_{\bar{X}_L}|$$
$$\leq \underbrace{\frac{\beta_{lw}\delta_W\left(C_l+\alpha C^d\right)+\beta_{lw}\bar{X}_W\alpha\left(\phi+\epsilon_C\right)}{\left(C_l+\alpha C^d\right)^2-\alpha^2(\phi+\epsilon_C)^2}}_{\delta_L}. \tag{52}$$

When the error terms $\hat{e}$ and $\hat{e}_C$ are zero-mean, i.e., $E[\hat{e}] = E[\hat{e}_C] = 0$, the average pathogen levels can be computed from the centers derived in Eqs. (48) and (52) as

$$X_{W_{ss}} = \frac{\beta_{ws}}{(\beta_{lw}\frac{L}{V}+\alpha C^d)} \text{ and } X_{L_{ss}} = \frac{\beta_{lw}X_{W_{ss}}}{\left(C_l+\alpha C^d\right)}. \tag{53}$$

□

Remark 5. Eqs. (42) and (43) show that terminal pathogen concentration intervals for water and lettuce can be computed by knowing the prescribed FC concentration in the water tank C^d and ultimate bounding radii ϕ and ϵ_C. Referring to Eq. (44), the expected pathogen levels can be predicted from the target FC if the errors have zero mean. These average levels and bounds depend on the shed rate of *E. coli*. The predicted levels and bounds change if β_{ws} changes.

4. Simulation results

This section verifies the effectiveness of the proposed NI-based HEKF/RASM algorithm by performing simulation studies on the produce wash system with nominal parameters presented in [14,38].

4.1. Desired FC concentration and initialization

For no pathogen survival, the desired FC concentration should be above 10 mg/L [23]; *E. coli O157:H7* cannot be detected on washed produce when the FC concentration in the wash water is above 10 mg/L. Three levels of the desired FC concentration ($C^d = [5, 10, 15](mg/L)$) are tested for the system to see how the pathogen levels change based on FC concentrations. The design parameters are set to $\lambda = 2$ and $k_{d_0} = 1$. The width of saturation function is adjusted depending on the target FC concentration as

$$\phi = 0.5 + 0.1C^d \tag{54}$$

implying that ϕ is chosen as 10% of C^d plus a constant considering the noise effects[3]Design parameters prioritize FCIR chattering-free and tracking performance. The initial condition of the system states is chosen as $[O(0), C(0), X_W(0), X_L(0)]^T = [350, 2, 0.7, 0.05]^T$ and differs from the filter initial condition, $[\hat{O}(0), \hat{C}(0), \hat{X}_W(0), \hat{X}_L(0)]^T = [300, 0, 0, 0]^T$, and all desired FC concentration levels. The initial covariance of the estimation is chosen as $P_0^+ = 10I$. The simulation runs for 36 min, which is equivalent to washing 1620 kg of lettuce [37].

4.2. State estimation

This section presents the results for the NI-based HEKF algorithm of Section 2.2, which simultaneously identifies the process and measurement noise statistics (filter noises), and estimates the system states under the proposed closed-loop control. Using the experimental data from a commercial double wash system in a commercial pilot plant (New Leaf Food Safety Solutions, LLC, in Salinas, CA), the covariance matrices of the system (used in Eq. (2)) are identified as $Q_s = \text{diag}(420, 0.4, 1.6, 1.2)$ and $R_{s_k} = 1$. The noise identification algorithm optimizes the covariance matrices of the filter (used in Eqs. (4) and (5)) as $Q_f = \text{diag}(700, 0.1, 1.9, 1.9)$ and $R_{f_k} = 1.2$.

Fig. 2 compares the actual states of the wash system with the estimated states using the NI-based HEKF/RASM algorithm. The proposed algorithm accurately estimates the wash system states for different C^d levels. Fig. 2 shows that when the FC concentration is regulated to 5 mg/L, the pathogen levels are relatively high.

[3] The parameter ϕ is different for different desired FC concentration as $\phi_{C^d=5} = 1$, $\phi_{C^d=10} = 1.5$, and $\phi_{C^d=15} = 2$.

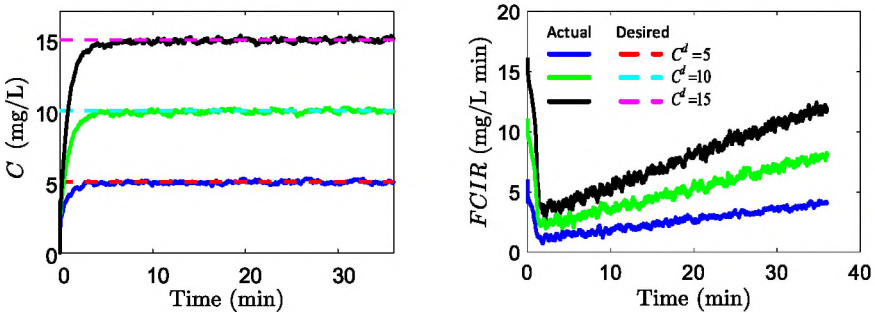

Fig. 3. FC tracking performance and the required FCIR.

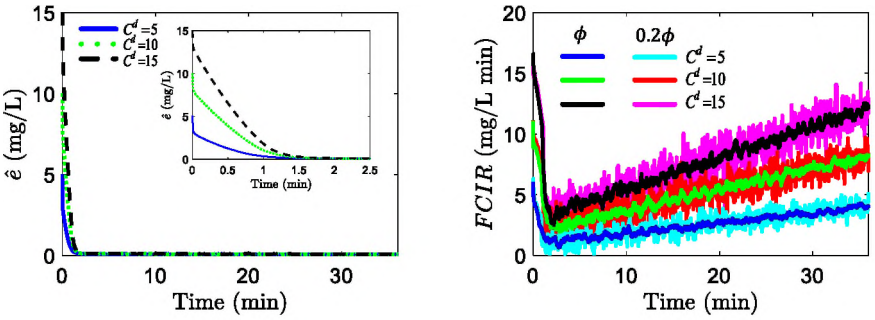

Fig. 4. Average RMSE_t^C of 100 Monte Carlo simulations (left figure) and the FCIR comparison between the controller using the width of saturation function ϕ suggested in Eq. (54) and the controller using 0.2 times 20%ϕ (right figure).

When the FC concentration increases to 10 and 15 mg/L, the *E. coli O157:H7* levels go down. In particular, for 15 mg/L FC concentration, *E. coli O157:H7* both in the water and on the lettuce are sufficiently killed (e.g., below the detection limits of 0.36 MPN/ml for the water and 0.36 MPN/g for the lettuce [21]) resulting in minimal pathogen cross-contamination.

4.3. FC concentration control

This section shows the FC concentration tracking performance and the required FCIR generated by the proposed closed-loop controller. Fig. 3 illustrates the FC concentration tracking responses, when the proposed controller is used. The actual[4] FC of the wash system accurately tracks different FC commands even when the initial value of the FC in the wash tank is zero. Fig. 3 also shows the required FC injection rates for different FC concentration levels, for which a higher FCIR is required to ensure a higher sustained FC concentration in the wash water. When the fresh-cut produce load increases, the required FCIR proportionally increases. Consequently, the FC concentration level remains unchanged in the water resulting in a constant level of pathogens in the water and on the lettuce (Fig. 2).

Fig. 4 shows the average RMSE_t^C (root mean square error of the FC tracking) from 100 Monte Carlo simulations each with a 36 min simulation time. This figure illustrates that the proposed controller provides accurate FC tracking for all three target FC levels. To shed some light on the Remark 3, Fig. 4 also demonstrates the effects of the width of saturation function ϕ on the FCIR solutions. Although experiments show that the controller with $\phi_s = 0.2\phi$ ($\phi_s = 0.2, 0.3, 0.4$ for $C^d = 5, 10, 15$, respectively) enhances the tracking performance up to 5% for all three levels of the desired FC concentration, it can be seen from this figure that decreasing ϕ causes undesirable oscillations in the FCIR solutions. This phenomenon (oscillations) is known as 'chattering' and may be harmful for the moving parts of the chlorine actuator. These oscillations can be properly reduced by adjusting the design parameter ϕ as mentioned in Remark 3. Fig. 4 shows that when the controller derives the parameter ϕ from Eq. (54), a reasonable trade off between tracking performance and chattering is made resulting in chattering-free FCIR solutions.

4.4. Pathogen levels

This section supports Theorem 2, in which the steady-state *E. coli O157:H7* levels and the corresponding intervals are computed from Eqs. (42)–(44). Fig. 5 compares the actual pathogen levels with the steady-state ones. This figure confirms that both pathogen levels in the water and on the lettuce converge to their predicted values, and stay bounded by their calculated intervals for all different C^d levels.

4.5. Numerical evaluation

This section shows that when the proposed controller regulates the FC concentration level at 15 mg/L, no pathogen can be detected in the water and on the lettuce. Table 1 lists RMSE value for state estimation, RMSE_s, RMSE value of tracking performance, RMSE_t, RMS value of the FCIR, RMS_u, steady state value of the pathogen in the water, X_W^{ss}, and steady state value of the pathogen on the lettuce, X_L^{ss}, for the wash system using the proposed controller. Since, in this paper, the FC concentration in the wash solution is between 5 mg/L and 15 mg/L (in steady state) during the washing process, Table 1 is comparable with Table 3 of [21], in which the relationship between the *E. coli O157:H7* survival and the FC concentration level was numerically reported for different C^d solutions from 5- to 25-mg/L.

This table shows that as the FC concentration level increases, the estimation performance of O, X_W, and X_L improves while chlorine estimation slightly degrades. The RMSE value of FC tracking

[4] The word "actual" stands for the variables that are generated from the model of Eq. (1), while the word "estimated" represents the variables that are estimated based on the model and the experimental data as explained in Section 2.2.

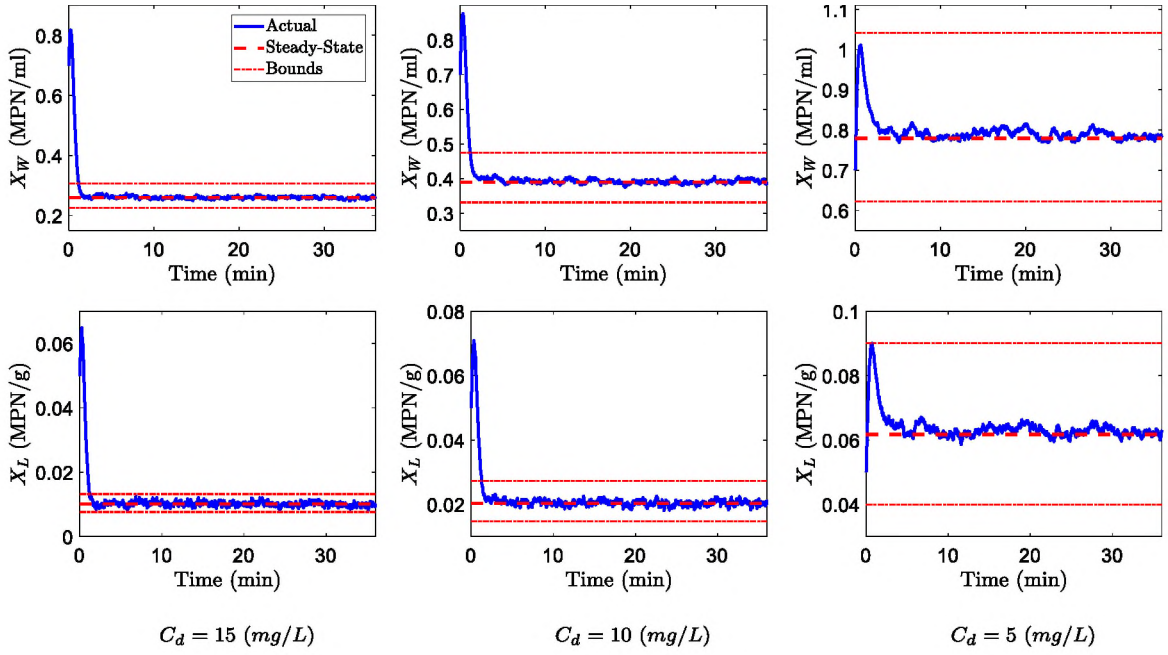

Fig. 5. The actual and steady-state *E. coli O157:H7* for different desired FC concentration. The dash-dot lines show the computed bounds for the pathogen levels. The y-axis scales differ for the three target concentrations.

Table 1
Tracking and estimation performances, and pathogen levels for different C^d solutions i.e., 5- to 25-mg/L (comparable to Table 3 of [21]), where $\mathcal{ND}$ denotes "not detected" at a detection level of 0.36 MPN/ml in water and 0.36 MPN/g on lettuce. Better values for each metric are underlined.

C^d	RMSE_s^O	RMSE_s^C	$\text{RMSE}_s^{X_W}$	$\text{RMSE}_s^{X_L}$	RMSE_t^C	RMS_u	X_W^{ss}	X_L^{ss}
5	29.690	0.132	0.075	0.008	0.326	2.766	0.787	$0.062^{\mathcal{ND}}$
10	20.750	0.145	0.065	0.007	0.788	5.600	0.392	$0.020^{\mathcal{ND}}$
15	18.180	0.164	0.057	0.005	1.267	8.540	$0.259^{\mathcal{ND}}$	$0.009^{\mathcal{ND}}$

increases with the increase in FC concentration level, whereas the FCIR must increase when the targeted FC is increased. The reason why RMSE_s^C and RMSE_t^C increase with the increase of targeted FC level stems from the larger initial condition mismatch between actual and estimated states with desired FC value. In addition, increasing the FC concentration in the wash water by 10 mg/L (from 5 and 15 mg/L) results in decreasing pathogen levels in the water by 67% and on the lettuce by 85%. In particular, when the FC concentration level reaches 15 mg/L, there is no detectable *E. coli O157:H7* in the wash water and on the lettuce (pathogen levels are below the detection level of 0.36 MPN/ml in water and 0.36 MPN/g on lettuce). When the FC concentration target is 15 mg/L, pathogen cross-contamination is effectively eliminated from the wash system.

4.6. Robustness in the presence of parameter uncertainties

In this section, system parameters are deviated from their nominal values from −50% to +50% with a resolution of 0.05 to see how the system reacts to parameter uncertainties under the proposed controller. Fig. 6 illustrates that RMSE_t^C increases as $\Delta\theta$ is iteratively perturbed, for all different levels of the targeted FC concentration. Table 2 shows that although for all C^d values, tracking performance deteriorates when system parameters are perturbed by ± 50%, RMSE_t^C is impacted by the perturbation much less as C^d increases. For instance, when FC concentration is targeted at 15 mg/L, the tracking performance degrades by only 6% and 10% for +50% and −50% parameter uncertainty respectively. Fig. 6 also shows that the FCIR linearly increases as $\Delta\theta$ increases. However,

Table 2
Controller performance in the presence of parameter uncertainties. The table shows percent chance in values when the system parameters deviate by ± 50%, where the plus sign shows a deterioration and the minus sign shows an improvement versus the controller performance with the nominal values.

	$\Delta\theta(\%)$	$C^d = 5$	$C^d = 10$	$C^d = 15$
RMSE_t^C	+50	+33%	+11%	+6%
	−50	+40%	+13%	+10%
RMS_u	+50	+12%	+8%	+2%
	−50	−19%	−12%	−11%

according to Table 2, when C^d is regulated at 15 mg/L, the required FCIR only increases by 2% due to the +50% parameter perturbation.

4.7. Controller performance in the presence of the chlorine actuator failure

FC control actuator failures may cause an unknown disturbance and negatively impact wash system performance. In this section, an unknown time-varying disturbance $u_d(t)$ is applied to the wash system and performance of the control law of Eq. (8) along with the adaptation mechanism of Eq. (10) is evaluated to see how the proposed controller compensates for the disturbance. For the sake of illustration of the adaptation mechanism against the actuator failures, the FC concentration is targeted at $C^d = 5$ based on which ϕ is computed using Eq. (54) while other design parameters remain unchanged. The disturbance $u_d(t)$ takes values +5 and −7 in two time periods $t \in [8, 10]$sec and $t \in [23, 27]$sec respectively.

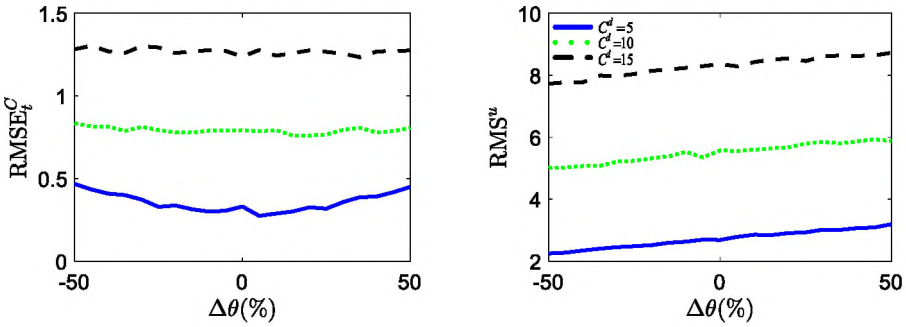

Fig. 6. Tracking performance and required FCIR in the presence of parameter uncertainties.

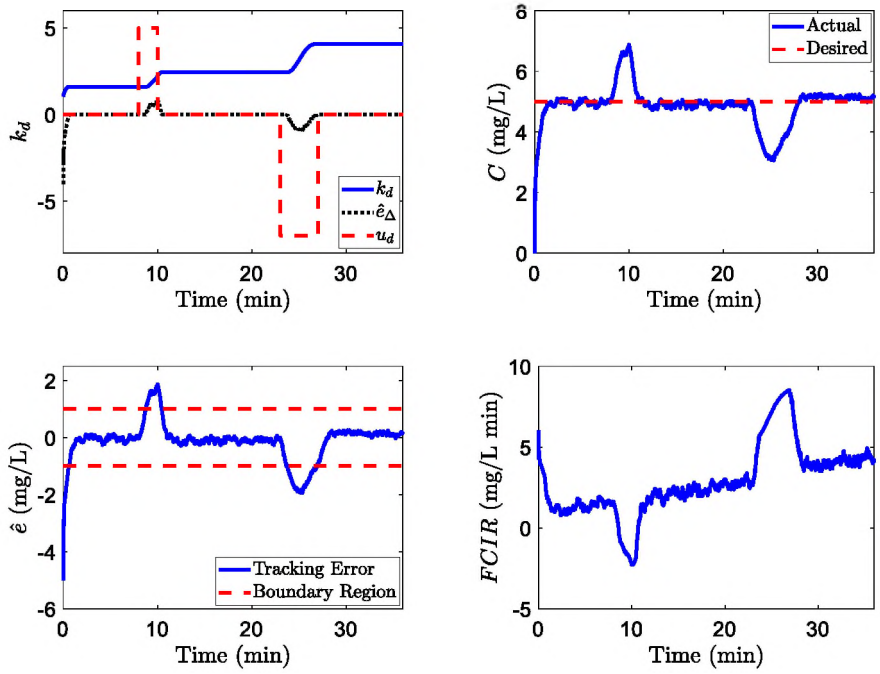

Fig. 7. Controller performance in the presence of the unknown disturbance $u_d(t)$. The disturbance $u_d(t)$ takes values $+5$ and -7 in two time periods $t \in [8, 10]$ min and $t \in [23, 27]$ min respectively.

Fig. 7 illustrates the time-varying disturbance $u_d(t)$, FC tracking performance, and required FCIR when FC is targeted at 5 mg/L. It is seen that in the absence of the disturbance, $\hat{e}_\Delta = 0$, adaptation of Eq. (10) is off, and in turn k_d is constant. However, when the disturbance is encountered for $t \in [8, 10]$ min and $t \in [23, 27]$ min, the error trajectory $\hat{e}$ leaves the boundary layer, $\hat{e}_\Delta$ deviates, and the controller gain updates to compensate for the disturbance. This figure also illustrates that although the FC concentration deviates from the desired FC at the disturbance exposure, it quickly converges with k_d settling once the error lies within the boundary layer region. The net effect is to modulate the FCIR to drive the FC concentration to its target value.

Fig. 8 compares the actual system states with the estimated ones when the disturbance appears. When this disturbance emerges, the estimated states deviate but then return to the actual states. The estimated COD in the water wash has a more sluggish convergence back to the actual COD. Fig. 8 also shows that although the COD dynamic is independent of the FC dynamic and in turn of $u_d(t)$, the estimated COD is effected when the actuator fails. This is because the NI-based HEKF algorithm estimates all the states by measuring the actual FC whose dynamic is effected by $u_d(t)$. Thus the estimated COD deviates from the true values when the actuator failure happens.

To further highlight the benefit of the proposed adaptation mechanism of Eq. (10), experiments are carried out with a constant-gain controller, $k_d = k_{d_0}$[5], when the unknown disturbance u_d is applied two times during the simulation while the FC concentration is targeted at 5 *mg/L*. Fig. 9 shows that under the constant-gain controller, the FC concentration tracking performance is degraded by 46% over the proposed controller with time-varying control gain (see Table 3). In addition, the peak and steady state pathogen levels in the water and on the lettuce are dramatically increased with the constant-gain controller. Comparing Figs. 8 and 9 demonstrates that under the constant-gain controller, the peak pathogen levels increase from 4 to 31 (MPN/ml) for X_W and from 0.54 to 4.9 (MPN/g) for X_L (Table 3), resulting in a suddenly large pathogen level and also deteriorating the estimation performance.

Table 3 lists RMSE$_t$, X_W^{ss}, X_L^{ss}, and the peak pathogen levels, $X_{W_{\max}}$ and $X_{L_{\max}}$, for all three levels of the desired FC concentration under both proposed and constant-gain controllers. It can be inferred from this table that the proposed controller with the adap-

[5] As the scale of the actuator failure is unknown, the constant control gain is guessed as $k_d = k_{d_0} = 1$.

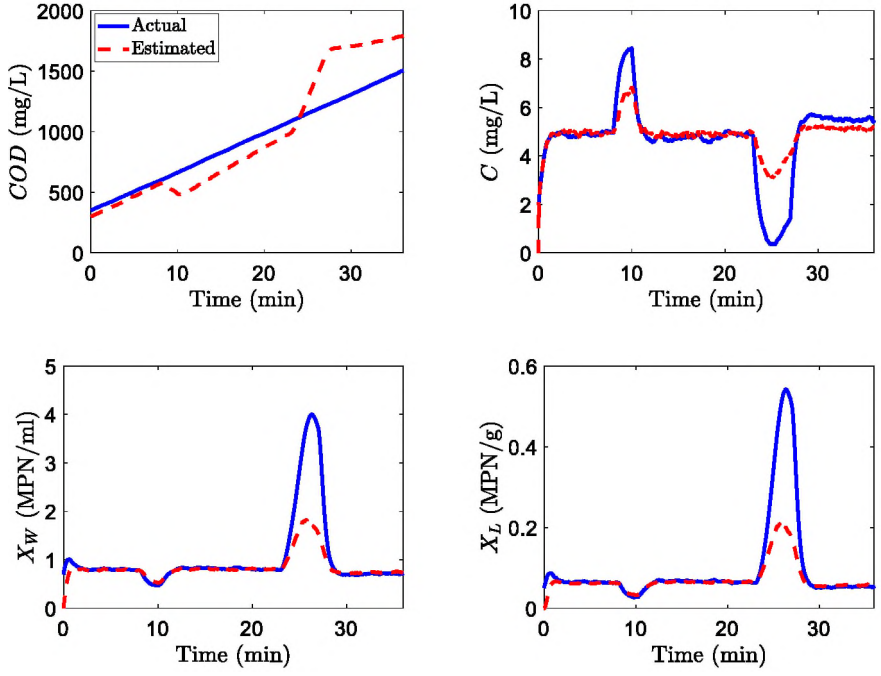

Fig. 8. State estimation performance in the presence of the unknown disturbance $u_d(t)$.

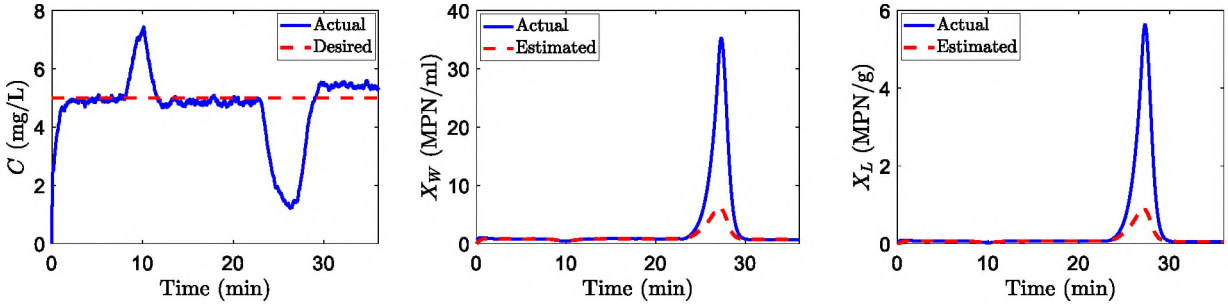

Fig. 9. Tracking performance and pathogen levels in the presence of the unknown disturbance $u_d(t)$ for the constant-gain controller.

Table 3
Performance comparison between our proposed approach and the constant-gain controller for different levels of the desired FC concentration in the presence of the unknown disturbances, where $\mathcal{ND}$ stands for "not detected" at a detection level of 0.36 MPN/ml in water and 0.36 MPN/g on lettuce. Better values for each metric are underlined.

C^d	Controller	RMSE_t^C	X_W^{ss}	X_L^{ss}	$X_{W_{\max}}$	$X_{L_{\max}}$
5	Proposed	0.660	1.270	0.131$^{\mathcal{ND}}$	4.00	0.541
	Constant gain	1.230	4.060	0.585	31.251	4.978
10	Proposed	0.941	0.421	0.024$^{\mathcal{ND}}$	0.880	0.070$^{\mathcal{ND}}$
	Constant gain	1.500	0.477	0.029$^{\mathcal{ND}}$	0.950	0.080$^{\mathcal{ND}}$
15	Proposed	1.383	0.262$^{\mathcal{ND}}$	0.009$^{\mathcal{ND}}$	0.811	0.060$^{\mathcal{ND}}$
	Constant gain	1.930	0.280$^{\mathcal{ND}}$	0.013$^{\mathcal{ND}}$	0.829	0.069$^{\mathcal{ND}}$

tation mechanism presented in Eq. (10) outperforms the constant-gain controller in the presence of the FC control actuator failures under different levels of C^d with regard to all design specifications such as pathogen minimization and FC concentration tracking performance.

5. Effects of incoming pre-wash pathogen levels

This section analyses the effects of the pathogen-to-water shedding rate on the pathogen levels during washing. The input rate of the pathogen into the water β_{ws} is the first term in the water pathogen contamination dynamic of Eq. (1c). Based on the observations in [14,37], β_{ws} is approximately constant during washing (assuming a constant incoming microbial load on the pathogen delivery vehicle). An important application of the developed model and FC controller concerns the maximum input rate of *E. coli* into the wash water with regards to (i) whether or not pathogen levels remain below the prescribed detection level in the water and (ii) the possibility of significant cross-contamination from water to lettuce.

Table 4 shows that the maximum value of β_{ws} for no *E. coli O157:H7* survival both in the water and on the lettuce is $\beta_{ws}^{max} = 2.63$ $(MPN/(ml\,\text{min}))$, which is +35% variation of its nominal value $\beta_{ws} = 1.95$ $(MPN/(ml\,\text{min}))$. Comparing Table 1 with Table 4 shows that when β_{ws} increases by +35%, X_W^{ss} and X_L^{ss} increase by 35% and 44% respectively. With more than +35% deviation on β_{ws}, although the steady state pathogen level on lettuce remains below the detection level of 0.36 *MPN/ml*, the steady state pathogen level in water exceeds the level. Table 5 shows that the maximum value of β_{ws} for no *E. coli O157:H7* survival on the lettuce is $\beta_{ws}^{max} = 68.25$ $(MPN/(ml\,\text{min}))$, which is +3400% variation of its nominal value. However, with this deviation of β_{ws}, the steady state pathogen level in water obviously exceeds the detection threshold.

In light of the above discussion, it is important to point out that given pathogen-produce specific wash processing data (similar to that in [37]), we can quantifiably link β_{ws} to specifics

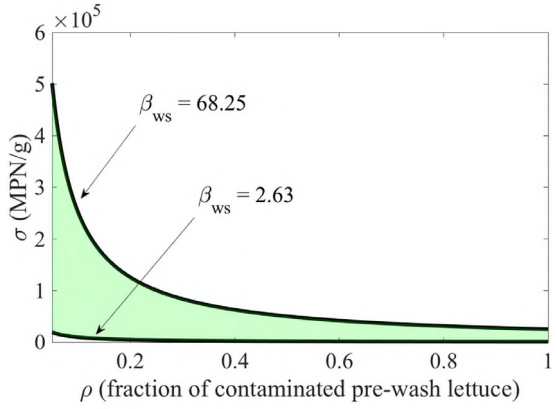

Fig. 10. Management guidelines for controlling cross-contamination. σ (MPN/g) is the mean pathogen level on contaminated pre-wash lettuce and ρ is the fraction of pre-wash contaminated lettuce relative to total incoming pre-wash lettuce. Building off the results in Tables 4 and 5 and Eq. (58), the region between the curves (or below the upper curve) indicates when *E. coli* cross-contamination via wash water is controlled (i.e. $\beta_{ws} < 68.25$) given that $C^d = 15$ (mg/L).

concerning pathogen concentration and prevalence on pre-washed produce, thus informing pre-processing management to minimize cross-contamination during the wash step. In particular, we can express β_{ws} $(MPN/(ml\,\min))$ as follows (see [14] for similar calculation):

$$\beta_{ws} = \frac{(\sigma - X_l)R_{lt}}{V}, \tag{55}$$

where R_{lt} (g/min) is rate of contaminated lettuce coming into the tank; σ (MPN/g) represents the mean pathogen level on contaminated pre-wash lettuce; X_l (MPN/g) represents the mean pathogen level remaining on initially contaminated lettuce during washing; V (ml) is volume of wash tank. To find an explicit relationship between β_{ws} and σ, we can reasonably approximate X_l as a function of σ as follows:

$$X_l = \sigma e^{-0.5b}, \tag{56}$$

where the shed rate b can be calculated by a given pair of (σ, X_l) and 0.5 min is the average dwell time of the produce in the wash tank.

Substituting Eq. (56) into Eq. (55), β_{ws} can be presented as an explicit function of σ

$$\beta_{ws} = \sigma \frac{(1 - e^{-0.5b})R_{lt}}{V}. \tag{57}$$

Based on experimental data in Table 2, column 3 of [21], and data presented in Figure 1 of [44], we calculate that $b = 0.43 \pm 0.1$ (1/min). Furthermore, we express $R_{lt} = \rho N_l$, where $\rho \in (0, 1)$ indicates the fraction of incoming lettuce that is contaminated and N_l (g/min) is the input rate of lettuce into the wash tank. Therefore, we have that

$$\beta_{ws} = \sigma \frac{(1 - e^{-0.5b})\rho N_l}{V}. \tag{58}$$

Using the fact that $N_l = 45,000$ (g/min), $V = 3.2 \times 10^6$ ml (coming from [14,37]), and $b = 0.43$ (1/min), we want to know when $\beta_{ws} \in [2.63, 68.25]$ given ρ and σ. Fig. 10 illustrates a basic guide for controlling water mediated cross-contamination. Essentially, if the pair (ρ, σ), that is the fraction of incoming lettuce that is contaminated with average pathogen level σ, lies in the region between the two curves (or below the upper curve), using $C^d = 15$ (mg/L) for chlorine control indicates that on average, *E. coli* levels on post-wash lettuce (due to cross-contamination via water) will be below the detection limit. In particular, this says two things: i) on average, contaminated pre-wash lettuce will not leave the wash tank more contaminated and ii) if uncontaminated pre-wash lettuce picks up *E. coli* from the wash water the resulting level (on average) will be below the detection limit of 0.36 MPN/g. Notice that the water to lettuce transfer rate relies on the assumption of complete mixing (refer to the β_{lw} terms in model (1)), indicating that Fig. 10 provides guidelines to control the "worst case" scenario for "averaged" dynamics describing water mediated cross-contamination. Finally, it is important to mention that since the produce to water ratio in the tank is quite low (0.0061 (kg/L)), pathogen transfer due to direct produce to produce contact during washing is most likely insignificant as compared with the cross-contamination dynamic via contaminated water [19,21,44].

Table 4
Tracking and estimation performances, and pathogen levels for different input rates of *E. coli* at $C^d = 15$ mg/L with detection level of 0.36 MPN/ml in water and 0.36 MPN/g on lettuce.

β_{ws}	$RMSE_s^O$	$RMSE_s^C$	$RMSE_s^{X_W}$	$RMSE_s^{X_L}$	$RMSE_t^C$	RMS_u	X_W^{ss}	X_L^{ss}
3.00	20.301	0.131	0.057	0.005	1.293	8.290	0.404	$0.015^{N\mathcal{D}}$
2.82	18.057	0.120	0.057	0.005	1.290	8.231	0.378	$0.014^{N\mathcal{D}}$
2.63	18.212	0.129	0.057	0.005	1.276	8.225	$0.351^{N\mathcal{D}}$	$0.013^{N\mathcal{D}}$

Table 5
Tracking and estimation performances, and pathogen levels for different input rates of *E. coli* at $C^d = 15$ mg/L only considering a detection level of 0.36 MPN/g on lettuce.

β_{ws}	$RMSE_s^O$	$RMSE_s^C$	$RMSE_s^{X_W}$	$RMSE_s^{X_L}$	$RMSE_t^C$	RMS_u	X_W^{ss}	X_L^{ss}
79.95	20.176	0.130	0.115	0.009	1.286	8.216	10.651	0.412
72.15	18.083	0.148	0.119	0.010	1.270	8.368	9.645	0.374
68.25	19.412	0.156	0.117	0.009	1.267	8.288	9.128	$0.355^{N\mathcal{D}}$

6. Conclusions and future work

6.1. Conclusions

Experiments in [37] show that rapid input of organic load into the wash system decreases the FC level resulting in the potential for contaminated produce. In order to reduce FC variability during the washing process, a sufficient level of the FCIR must be injected into the wash tank to stabilize the FC concentration level and in turn reduce the risk of contaminated fresh produce. While on-line chlorine control is able to stabilize the FC level in the wash water, the challenge is that not only real-time measurements may not be available nor practical to obtain, but also noise statistics may be unknown. Since the existing mathematical model of the wash system is a simplified version of the actual system, the approximated model always contains modeling errors. In addition, chlorine actuators may not be able to consistently fulfill a sufficient FCIR due to actuator failure or faults.

In light of the aforementioned factors, FC control in produce wash systems with modeling errors and disturbances is a challenging task. Motivated by these issues, this paper presented a RASM control approach for a wash produce system while the system states were estimated using a HEKF and the noise statistics were identified by a NI algorithm. The resulting structure stabilized the FC concentration in the wash water and minimized the pathogen levels both in the wash water and on produce in the wash tank as fresh-cut produce was continually introduced to the wash tank. Stability of the proposed system was proved by the Lyapunov framework and the Barbalat's lemma, and the steady state pathogen levels were successfully predicted. In addition, simulation studies demonstrated that using the proposed algorithm, the system states are successfully estimated and FC concentration accurately tracks the desired FC level. According to the results, no *E. coli O157:H7* was detected when the FC level was targeted at

15 mg/L. Two robustness analyses showed that the proposed controller is able to compensate for possible chlorine actuator failures and system parameter uncertainties. In addition, simulation results illustrated that the proposed controller outperforms the baseline constant-gain controller providing a stronger robustification in the presence of chlorine actuator failure. Finally, our modeling/control approach provides cross-contamination management insight regarding the prevalence and mean pathogen levels of incoming pre-wash lettuce with respect to regulating FC levels in the wash tank at 15 mg/L.

6.2. Future work

In terms of future studies, the following items will be considered:

(1) In this paper, the FC concentration in the wash water was stabilized in the presence of unknown actuator failures and unmodeled dynamics. In order to enhance the model for the control structure, unmodeled neglected dynamics, such as breakpoint phenomena as well as the concentrations of chlorine by-products would be important to include explicitly. However, direct experimentation is needed to inform these dynamics (at near commercial scale) as well as the anti-microbial capacity of observed chlorine by-products.
(2) Although the FC concentration was controlled in this paper, minimization of the required FCIR has not been taken into account. In future work, optimization will be conducted to search for the optimal FCIR to achieve several specifications at the same time: FC concentration stabilization, optimization of the FC injection rate to the water tank, and minimization of the pathogen levels in the water and thus minimization of pathogen transfer (via water) to lettuce during washing.
(3) This paper estimated the system states with the assumption of Gaussian noise, for which the EKF is optimal. However, this notion may not hold during actual washing, so future studies will involve the estimation of system states in the presence of unknown non-Gaussian noise.
(4) Although the results showed that the proposed controller enables the system to manage the effect of potential actuator failure on FC levels in the wash water, the pathogen levels exceeded the detection levels (0.36 MPN/ml in water and 0.36 MPN/g on lettuce) as illustrated in Fig. 8. Future work is planned to design a controller such that the pathogens are maintained below such detection levels even when actuator failures are encountered. This task promises to create a safe control structure in the sense that *E. coli O157:H7* levels are consistently kept below a specified detection level.
(5) Finally, we discuss the need for specific data collection under the headings in the following two sections.

Management insight to minimize cross-contamination

Given $C^d = 15$ (mg/L), Fig. 10 illustrates that if the pair (ρ, σ) is below the $\beta_{ws} = 68.25$ curve, pathogen binding (via water) to uncontaminated pre-wash lettuce is effectively eliminated. Note that in general, ρ (fraction of pre-wash lettuce that is contaminated) and σ (average pathogen level of pre-wash contaminated lettuce), will vary in time. In this context, however, the results in Fig. 10 still hold as long as $(\rho(t), \sigma(t))$ remains in the region below the $\beta_{ws} = 68.25$ curve, and thus provide key management thresholds for addressing cross-contamination during washing.

In addition, it is important to mention that the shed rate b (1/min) used in Eq. (58) was determined from data at the bench-top scale [21]. It may be that this is an underestimate for b as one would expect shear forces in commercial wash processes to exceed the manual agitation used in [21]. This suggests the import of conducting pilot scale wash studies to determine the shed rate of pathogens from produce in the context of a variety of pathogen-produce pairs. This data combined with our model and chlorine control law will provide a further measure of validation for using the results in Fig. 10 to inform cross-contamination management.

6.2.1. pH control

Industry leaders that utilize high volume fresh-cut produce washing processes understand that pH is a critical control point for eliminating cross-contamination. Fundamentally, this is based on the fact that the concentration of hypochlorous acid, the most effective form of FC in terms of pathogen elimination, is highest when the pH < 6.5 [45]. Notice that the results in this paper rely on data and model forms in the context of wash water that has pH close to 6.5 during the 36 min wash process [37]. However, controlling pH in a commercial, high volume wash setting is still a technical challenge. For instance, in a recent commercial scale produce wash study by López-Gálvez et al. [46], the pH ranged between 4.2 and 8.3 across all data sets. Because the concentration of hypochlorous acid depends on the pH (and temperature) of the wash water, an effective FC control law should explicitly account for pH dynamics. However, more research is needed in terms of mathematically describing the chemistry involved in the interplay between FC and pH dynamics with regards to various fresh-cut produce commodities.

Declaration of Competing Interest

None.

References

[1] C. Arnade, F. Kuchler, L. Calvin, The changing role of consumers and suppliers in a food safety event: the 2006 foodborne illness outbreak linked to spinach, Appl. Econ. 48 (25) (2016) 2354–2366, doi:10.1080/00036846.2015.1119793.
[2] R.M. Callejn, M.I. Rodrguez-Naranjo, C. Ubeda, R. Hornedo-Ortega, M.C. Garcia-Parrilla, A.M. Troncoso, Reported foodborne outbreaks due to fresh produce in the united states and european union: trends and causes, Foodborne Pathogens Disease 12 (1) (2015) 32–38, doi:10.1089/fpd.2014.1821.
[3] Y. Jung, H. Jang, K.R. Matthews, Effect of the food production chain from farm practices to vegetable processing on outbreak incidence, Microb. Biotechnol. 7 (6) (2014) 517–527, doi:10.1111/1751-7915.12178.
[4] Centers for disease control and prevention, (https://www.cdc.gov/ecoli/outbreaks.html).
[5] S. Park, B. Szonyi, R. Gautam, K. Nightingale, J. Anciso, R. Ivanek, Risk factors for microbial contamination in fruits and vegetables at the preharvest level: a systematic review, J. Food Protect. 75 (11) (2012) 2055–2081.
[6] X. Nou, Y. Luo, Whole-leaf wash improves chlorine efficacy for microbial reduction and prevents pathogen cross-contamination during fresh-cut lettuce processing, J. Food Sci. 75 (5) (2010) M283–M290.
[7] Y. Luo, Fresh-cut produce wash water reuse affects water quality and packaged product quality and microbial growth in romaine lettuce, HortScience 42 (6) (2007) 1413–1419.
[8] F.P. Rodrguez, D. Campos, E. Ryser, A. Buchholz, G. Posada-Izquierdo, B. Marks, G. Zurera, E. Todd, A mathematical risk model for escherichia coli o157:h7 cross-contamination of lettuce during processing, Food Microbiol. 28 (4) (2011) 694–701.
[9] C. Shen, Y. Luo, X. Nou, Q. Wang, P. Millner, Dynamic effects of free chlorine concentration, organic load, and exposure time on the inactivation of salmonella, escherichia coli o157:h7, and non-o157 shiga toxin producing e. coli, J. Food Protect. 76 (3) (2013) 386–393.
[10] F. Lpez-Glvez, J.A. Tudela, A. Allende, M.I. Gil, Microbial and chemical characterization of commercial washing lines of fresh produce highlights the need for process water control, Innovat. Food Sci. Emerging Technol. (2018), doi:10.1016/j.ifset.2018.05.002.
[11] D.F. Maffei, A.S. Sant'Ana, B.D. Franco, D.W. Schaffner, Quantitative assessment of the impact of cross-contamination during the washing step of ready-to-eat leafy greens on the risk of illness caused by salmonella, Food Res. Int. 92 (2017) 106–112.
[12] S.V. Haute, Y. Luo, I. Sampers, L. Mei, Z. Teng, B. Zhou, E. Bornhorst, Q. Wang, P. Millner, Can uv absorbance rapidly estimate the chlorine demand in wash water during fresh-cut produce washing processes? Postharvest Biol. Technol. 142 (2018) 19–27.
[13] M. Deborde, U. von Gunten, Reactions of chlorine with inorganic and organic compounds during water treatment kinetics and mechanisms: a critical review, Water Res. 42 (1) (2008) 13–51.

[14] D. Munther, Y. Luo, J. Wu, F.M. Magpantay, P. Srinivasan, A mathematical model for pathogen cross-contamination dynamics during produce wash, Food Microbiol. 51 (Supplement C) (2015) 101–107.
[15] M.I. Gil, A. Marn, S. Andujar, A. Allende, Should chlorate residues be of concern in fresh-cut salads? Food Control 60 (2016) 416–421.
[16] X. Chen, Y.-C. Hung, Effects of organic load, sanitizer ph and initial chlorine concentration of chlorine-based sanitizers on chlorine demand of fresh produce wash waters, Food Control 77 (2017) 96–101.
[17] S. Weng, Y. Luo, J. Li, B. Zhou, J.G. Jacangelo, K.J. Schwab, Assessment and speciation of chlorine demand in fresh-cut produce wash water, Food Control 60 (2016) 543–551.
[18] P.M. Toivonen, C. Lu, Differential quenching of free chlorine by organic compounds potentially exuded from injured plant tissues, Postharvest Biol. Technol. 86 (2013) 192–194.
[19] D. Gombas, Y. Luo, J. Brennan, G. Shergill, R. Petran, R. Walsh, H. Hau, K. Khurana, B. Zomorodi, J. Rosen, R. Varley, K. Deng, Guidelines to validate control of cross-contamination during washing of fresh-cut leafy vegetables, J. Food Protect. 80 (2) (2017) 312–330.
[20] S. Van Haute, I. Tryland, C. Escudero, M. Vanneste, I. Sampers, Chlorine dioxide as water disinfectant during fresh-cut iceberg lettuce washing : disinfectant demand, disinfection efficiency, and chlorite formation, LWT-Food Sci. Technol. 75 (2017) 301–304.
[21] Y. Luo, X. Nou, Y. Yang, I. Alegre, E. Turner, H. Feng, M. Abadias, W. Conway, Determination of free chlorine concentrations needed to prevent escherichia coli o157:h7 cross-contamination during fresh-cut produce wash, J. Food Protect. 74 (3) (2011) 352–358.
[22] V.M. Gmez-Lpez, A.-S. Lannoo, M.I. Gil, A. Allende, Minimum free chlorine residual level required for the inactivation of escherichia coli o157:h7 and trihalomethane generation during dynamic washing of fresh-cut spinach, Food Control 42 (Supplement C) (2014) 132–138.
[23] Y. Luo, B. Zhou, S.V. Haute, X. Nou, B. Zhang, Z. Teng, E.R. Turner, Q. Wang, P.D. Millner, Association between bacterial survival and free chlorine concentration during commercial fresh-cut produce wash operation, Food Microbiol. 70 (2018) 120–128.
[24] X. Chang, J.H. Park, P. Shi, Fuzzy resilient energy-to-peak filtering for continuous-time nonlinear systems, IEEE Trans. Fuzzy Syst. 25 (6) (2017) 1576–1588.
[25] X. Chang, G. Yang, Nonfragile H_∞ filtering of continuous-time fuzzy systems, IEEE Trans. Signal Process. 59 (4) (2011) 1528–1538.
[26] J.-J.E. Slotine, J.A. Coetsee, Adaptive sliding controller synthesis for non-linear systems, Int. J. Control 43 (6) (1984) 1631–1651.
[27] J. Huang, Z.H. Guan, T. Matsuno, T. Fukuda, K. Sekiyama, Sliding-mode velocity control of mobile-wheeled inverted-pendulum systems, IEEE Trans. Robot. 26 (4) (2010) 750–758.
[28] R. Xu, mitzgner, Sliding mode control of a class of underactuated systems, Automatica 44 (1) (2008) 233–241.
[29] N.I.C. Molina, J.P.V. Cunha, Non-collocated sliding mode control of partial differential equations for soil irrigation, J. Process Control 73 (2019) 1–8.
[30] C.-T. Chen, S.-T. Peng, Design of a sliding mode control system for chemical processes, J. Process Control 15 (5) (2005) 515–530.
[31] G. Herrmann, S.K. Spurgeon, C. Edwards, A model-based sliding mode control methodology applied to the HDA-plant, J. Process Control 13 (2) (2003) 129–138.
[32] W. Garcia-Gabin, F. Dorado, C. Bordons, Real-time implementation of a sliding mode controller for air supply on a pem fuel cell, J. Process Control 20 (3) (2010) 325–336.
[33] X. Zhao, X. Wang, S. Zhang, G. Zong, Adaptive neural backstepping control design for a class of nonsmooth nonlinear systems, IEEE Trans. Syst. Man Cybern. Syst. 49 (9) (2019) 1820–1831.
[34] X. Zhao, P. Shi, X. Zheng, Fuzzy adaptive control design and discretization for a class of nonlinear uncertain systems, IEEE Trans. Cybern. 46 (6) (2016) 1476–1483.
[35] X. Zhao, X. Wang, G. Zong, X. Zheng, Adaptive neural tracking control for switched high-order stochastic nonlinear systems, IEEE Trans. Cybern. 47 (10) (2017) 3088–3099.
[36] J.-J.E. Slotine, W. Li, Composite adaptive control of robot manipulators, Automatica 25 (4) (1989) 509–519.
[37] Y. Luo, X. Nou, P. Millner, B. Zhou, C. Shen, Y. Yang, Y. Wu, Q. Wang, H. Feng, D. Shelton, A pilot plant scale evaluation of a new process aid for enhancing chlorine efficacy against pathogen survival and cross-contamination during produce wash, Int. J. Food Microbiol. 158 (2) (2012) 133–139.
[38] V. Azimi, D. Munther, S.A. Fakoorian, T.T. Nguyen, D. Simon, Hybrid extended Kalman filtering and noise statistics optimization for produce wash state estimation, J. Food Eng. 212 (Supplement C) (2017) 136–145.
[39] D. Simon, Optimal State Estimation: Kalman, H-infinity, and Nonlinear Approaches, John Wiley & Sons, 2006.
[40] K. Reif, S. Gunther, E. Yaz, R. Unbehauen, Stochastic stability of the continuous-time extended Kalman filter, IEE Proc. Control Theory Appl. 147 (1) (2000) 45–52.
[41] S. Fakoorian, V. Azimi, M. Moosavi, H. Richter, D. Simon, Ground reaction force estimation in prosthetic legs with nonlinear Kalman filtering methods, ASME. J. Dyn. Sys., Meas., Control 139 (11) (2017) 111004–111004–11.
[42] V. Azimi, T. Shu, H. Zhao, R. Gehlhar, D. Simon, A.D. Ames, Model-based adaptive control of transfemoral prostheses: theory, simulation, and experiments, IEEE Trans. Syst. Man Cybern. Syst. (2019) 1–18, doi:10.1109/TSMC.2019.2896193.
[43] J.-J.E. Slotine, W. Li, Applied Nonlinear Control, Prentice-Hall, 1991.
[44] F. Lopez-Galvez, M.I. Gil, P. Truchado, M.V. Selma, A. Allende, Cross-contamination of fresh-cut lettuce after a short-term exposure during pre-washing cannot be controlled after subsequent washing with chlorine dioxide or sodium hypochlorite, Food Microbiol. 27 (2) (2010) 199–204.
[45] B.V. Corporation, White's Handbook of Chlorination and Alternative Disinfectants, John Wiley and Sons Ltd, 2010.
[46] F. Lopez-Galvez, J.A. Tudela, A. Allende, M.I. Gil, Microbial and chemical characterization of commercial washing lines of fresh produce highlights the need for process water control, Innovat. Food Sci. Emerg. Technol. (2018).
[47] V. Azimi, S.A. Fakoorian, T.T. Nguyen, D. Simon, Robust Adaptive Impedance Control With Application to a Transfemoral Prosthesis and Test Robot, Journal of Dynamic Systems, Measurement, and Control 140 (12) (2018).